

www.acsabm.org Article

Antibacterial, Anti-Inflammatory, and Antioxidant Cotton-Based Wound Dressing Coated with Chitosan/Cyclodextrin—Quercetin Inclusion Complex Nanofibers

Mohsen Alishahi, Ruobai Xiao, Melisa Kreismanis, Rimi Chowdhury, Mahmoud Aboelkheir, Serafina Lopez, Craig Altier, Lawrence J. Bonassar, Hongqing Shen, and Tamer Uyar*



Cite This: ACS Appl. Bio Mater. 2024, 7, 5662-5678

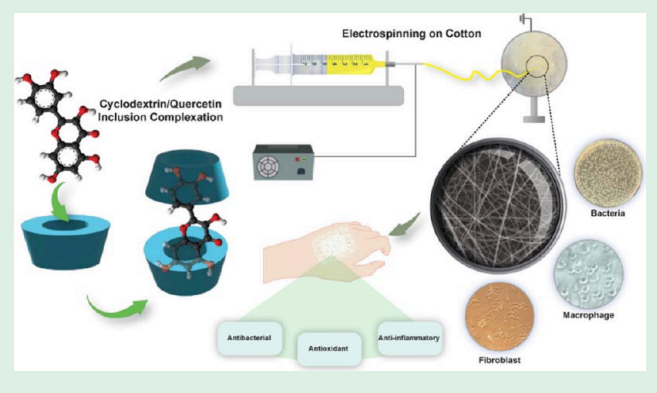


ACCESS

III Metrics & More

Article Recommendations

ABSTRACT: Quercetin, recognized for its antioxidant, anti-inflammatory, and antibacterial properties, faces limited biomedical application due to its low solubility. Cotton, a preferred wound dressing material over synthetic ones, lacks inherent antibacterial and wound-healing attributes and can benefit from quercetin features. This study explores the potential of overcoming these challenges through the inclusion complexation of quercetin with cyclodextrins (CDs) and the development of a nanofibrous coating on a cotton nonwoven textile. Hydroxypropyl-beta-cyclodextrin (HP- β -CD) and hydroxypropyl-gamma-cyclodextrin (HP- γ -CD) formed inclusion complexes of quercetin, with chitosan added to enhance antibacterial properties. Phase solubility results showed that inclusion complexation can enhance quercetin solubility up to



20 times, with HP- γ -CD forming a more stable inclusion complexation compared with HP- β -CD. Electrospinning of the nanofibers from HP- β -CD/Quercetin and HP- γ -CD/Quercetin aqueous solutions without the use of a polymeric matrix yielded a uniform, smooth fiber morphology. The structural and thermal analyses of the HP- β -CD/Quercetin and HP- γ -CD/Quercetin nanofibers confirmed the presence of inclusion complexes between quercetin and each of the CDs (HP- β -CD and HP- γ -CD). Moreover, HP- β -CD/Quercetin and HP- γ -CD/Quercetin and followed a fast-releasing profile of quercetin. Both HP- β -CD/Quercetin and HP- γ -CD/Quercetin nanofibers showed significantly higher antioxidant activity compared to pristine quercetin. The HP- β -CD/Quercetin and HP- γ -CD/Quercetin nanofibers also showed antibacterial activity, and with the addition of chitosan in the HP- γ -CD/Quercetin system, the Chitosan/HP- γ -CD/Quercetin nanofibers completely eliminated the investigated bacteria species. The nanofibers were nontoxic and well-tolerated by cells, and exploiting the quercetin and chitosan anti-inflammatory activities resulted in the downregulation of IL-6 and NO secretion in both immune as well as regenerative cells. Overall, CD inclusion complexation markedly enhances quercetin solubility, resulting in a biofunctional antioxidant, antibacterial, and anti-inflammatory wound dressing through a nanofibrous coating on cotton textiles.

KEYWORDS: Antibacterial, Anti-inflammatory, Antioxidant, Cotton, Cyclodextrin, Nanofiber, Quercetin, Wound dressing

1. INTRODUCTION

With the skin being the body's largest organ, it is particularly vulnerable to injury and wound development. In wound management, the use of dressings is a common approach to serve as a physical barrier against external elements. These dressings not only shield wounds from external factors but also play a crucial role in regulating wound moisture, absorbing exudate, and facilitating air transmission to the wound environment. Cotton as the most dominant cellulosic natural fiber stands out as the most prevalent traditional wound dressing used to protect the wound environment. The inherent natural properties of cotton make it a biocompatible and sustainable material to be applied in biomedical and

pharmaceutical fields.³ Besides the mentioned attributes, the physical characteristics of cotton, including its intricate structure, moisture retention capability, and comfort properties, have established its status as the most commonly utilized wound dressing.³

Received: June 4, 2024 Revised: July 21, 2024 Accepted: July 23, 2024 Published: August 4, 2024





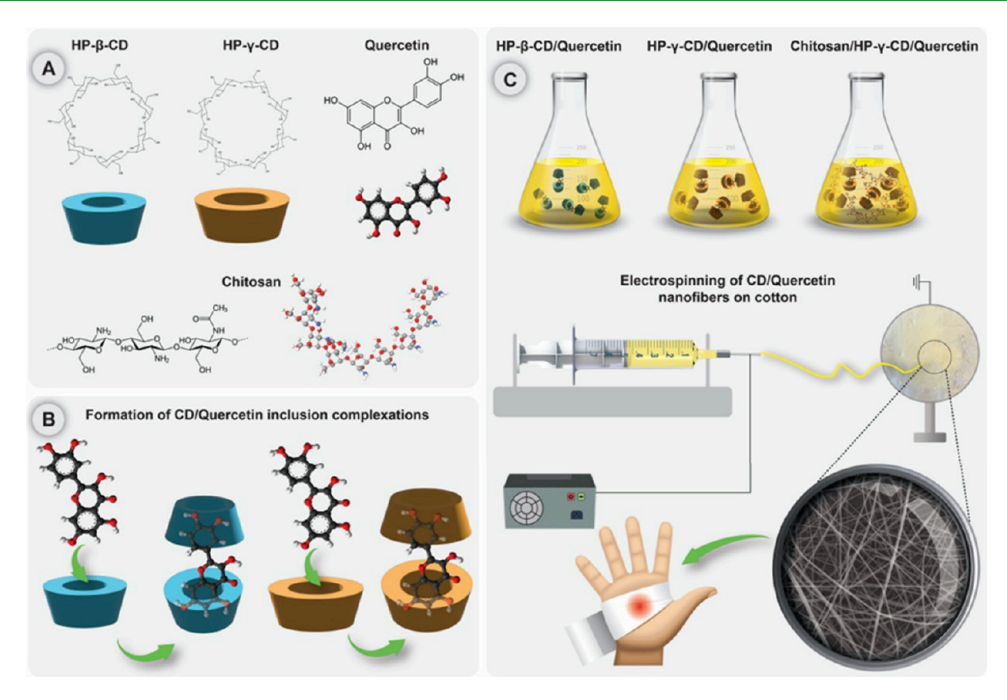


Figure 1. (A) Chemical structures of HP- β -CD, HP- γ -CD, quercetin, and chitosan. Schematic depictions of (B) the formation of inclusion complexes between quercetin and cyclodextrins (HP- β -CD and HP- γ -CD), and (C) the electrospinning fabrication of nanofibers with or without chitosan as a biofunctional nanofibrous coating onto cotton for wound dressing.

However, wound healing is a complex process consisting of multiple stages that can be interrupted due to factors such as infection, severe inflammation, oxidative stress, and preconditions like diabetes.^{4,5} Therefore, a suitable wound dressing should also prevent infection and oxidative stress and promote the healing process.⁶ Due to its limited bioactivity, cotton should be modified to develop antibacterial and wound-healing properties.³ Surface modifying the cotton substrate is a viable approach that is extensively explored, involving coatings with nanoparticles, hydrogel, and nanofibers. 9,10 Particularly, nanofibers play a major role in wound dressing due to their high surface-to-volume ratio, their similarity to the extracellular matrix, and their potential to mimic skin structure. 11,12 Besides, nanofibers can also provide the controlled release of drugs¹³ and result in the fabrication of multifunctional wound dressings.14

The incorporation of antibiotics is the main approach in providing antibacterial properties to wound dressings. However, besides the lack of wound-healing properties, using antibiotics can cause substantial side effects and raise the risk of drug resistance.¹⁵ Flavonoids as natural bioactives can overcome these complications besides providing antibacterial and wound-healing properties. 16,17 Quercetin, a natural pentahydroxyflavone, is among the most prevalent flavonoids present in a variety of fruits, vegetables, and leaves. 18 It has found widespread application in the food industry and pharmaceutics owing to its antioxidant, anti-inflammatory, antibacterial, antiobesity, and anticancer properties. 19,20 Quercetin is particularly known for its antioxidant properties through eliminating reactive oxidant species (ROS),²¹ regulating the level of glutathione, 22 and affecting the signal transduction pathways.²³ However, like other flavonoids, quercetin's low solubility and bioavailability limit its pharmaceutical applications. 19 Quercetin is also shown to moderate the secretion of pro-inflammatory agents like nitrite

(NO) and pro-inflammatory cytokines such as interleukin-6 (IL-6). 24,25

Not only for quercetin, the administration of low-soluble drugs is one of the main complications in pharmaceutics. Nanofibers are employed as a viable tool to enhance the solubility of drugs by co-dissolving them with polymers. However, it is challenging to enhance the solubility of some poorly water-soluble drugs due to the lack of suitable solvents, resulting in their diminished activity. ²⁸

The application of cyclodextrins (CDs) has become a very effective strategy to deal with the low solubility of quercetin. The capability of CDs, which are cyclic oligosaccharides with a hydrophobic core and a hydrophilic outside, to form noncovalent inclusion complexes is well-known.²⁹ This interaction improves the biocompounds' solubility, stability, and bioavailability and presents a viable way to increase biocompounds' therapeutic effect, as documented in our previous studies.^{30,31} Moreover, originating from natural sources, CDs are biocompatible.²⁹ The possibility to directly fabricate nanofibers from cyclodextrin inclusion complexes (CD-ICs) via electrospinning makes them well-suited for coating cotton nonwoven, as investigated in our recent study, 10 thereby enhancing their capability to be used as a wound dressing. The perspective of using CD/Quercetin inclusion complexes to improve quercetin's solubility was extensively investigated. It has been shown that the water solubility and antioxidant activity of quercetin were significantly enhanced by its inclusion complexation with methyl- β -CD.³² Another study corroborates improving the solubility and antioxidant activity of quercetin through the inclusion complexation with bis- β -CD.³³ Aiding from this improvement of solubility and stability, the development of CD/Quercetin nanofibers for different applications was investigated. Previously, we have shown that the fabrication of β -CD/Quercetin³⁰ and γ -CD/Quercetin³⁴ inclusion complexation and encapsulating them within electrospun poly(acrylic acid) (PAA) nanofibers³⁰ and zein nanofibers³⁴ could result in a high solubility of quercetin; these nanofibrous mats showed potent antioxidant activity and photostability of quercetin.³⁰

Besides its excellent antioxidant properties, quercetin shows moderate antibacterial activity, which can be further improved by adding another antibacterial natural biopolymer like chitosan. Therefore, in this study, the mentioned benefits of hydroxypropyl-beta-cyclodextrin (HP-β-CD) and hydroxypropyl-gamma-cyclodextrin (HP-γ-CD) were utilized to develop quercetin inclusion complexes. Subsequently, the inclusion complexes of HP-β-CD/Quercetin and HP-γ-CD/ Quercetin were electrospun to develop a nanofibrous coating on cotton nonwoven to fabricate a multifunctional wound dressing. After a performance evaluation between HP- β -CD/ Quercetin and HP-γ-CD/Quercetin systems, HP-γ-CD/ Quercetin was chosen, and chitosan was added to the HP-y-CD/Quercetin system to produce Chitosan/HP-γ-CD/Quercetin nanofibers for further improvement of the antibacterial activity of this nanofibrous coating. Figure 1 illustrates the outline of forming inclusion complexes between quercetin and CDs (HP- β -CD and HP- γ -CD) and electrospinning nanofibers from these HP-β-CD/Quercetin, HP-γ-CD/Quercetin, and Chitosan/HP-γ-CD/Quercetin systems. Following the optimization of electrospinning, uniform nanofibers were electrospun from these systems, and the resulting nanofibers were characterized to investigate their morphological, structural, biological, and pharmaco-technical properties.

2. MATERIALS AND METHODS

2.1. Materials. Hydroxypropyl-beta-cyclodextrin (HP- β -CD) (Cavasol W7 HP, with a degree of substitution of around 0.9) and hydroxypropyl-gamma-cyclodextrin (HP-γ-CD) (Cavasol W8 HP Pharma, with a degree of substitution of approximately 0.6) were kindly provided by Wacker Chemie AG (USA). Additionally, quercetin (quercetin hydrate, 95%, Thermo Scientific), chitosan (85% deacetylated, Alfa Aesar), methanol (≥99.8% purity by GC, Sigma-Aldrich), 2,2-diphenyl-1-picrylhydrazyl (DPPH, ≥97% purity, TCI America), dimethyl sulfoxide (DMSO, >99.9% purity, Sigma-Aldrich), sodium chloride (NaCl, >99% purity, Sigma-Aldrich), potassium phosphate monobasic (KH₂PO₄, ≥99.0% purity, Fisher Chemical), sodium phosphate dibasic heptahydrate (Na₂HPO₄, 98.0-102.0% purity, Fisher Chemical), o-phosphoric acid (85% purity by HPLC, Fisher Chemical), deuterated dimethyl sulfoxide (DMSO-d₆, purity 99.8%, Cambridge Isotope), and phosphatebuffered saline tablet (PBS, Sigma-Aldrich) were used as-received without further purification. The experiments were carried out using high-quality distilled water sourced from the Millipore Milli-Q ultrapure water system (Millipore, USA). We employed cotton nonwoven samples (50 GSM, 100% cotton, carded and hydroentangled substrates), which were provided as prototype samples from Cotton Incorporated (Cary, NC, USA).

2.2. Phase Solubility. The phase solubility examination of the HP- β -CD/Quercetin and HP- γ -CD/Quercetin systems adhered to a well-established methodology as previously used. ¹⁰ In separate glass vials, excessive quantities of quercetin and CD powder with a concentration spectrum spanning from 0 to 20 mM were introduced. Next, 5 mL of water was introduced to each vial. The sealed vials were then situated on an incubator shaker, safeguarded against exposure to light, and subjected to agitation for a continuous 24 h period at a temperature of 25 °C and a speed of 450 rpm. Afterward, the resulting mixtures were subjected to filtration using 0.45 μm PTFE filters (Thermo Scientific, Target2). The quantification of quercetin concentration was obtained UV—vis spectroscopically using a PerkinElmer Lambda 35 instrument, and these measurements were correlated with the established calibration curve for quercetin in PBS. This series of experiments was done in three replications, with the

mean absorbance values utilized for the generation of phase solubility diagrams. The binding constants (K_S) were calculated from the equation $K_S = \text{slope}/S_0(1-\text{slope})$, where S_0 is the intrinsic solubility of quercetin.

2.3. Investigating the Formation of Inclusion Complexations Using 2D-NMR. Rotating frame Overhauser effect spectroscopy (ROESY) was conducted to assess the formation of the inclusion complexations of HP- β -CD/Quercetin, and HP- γ -CD/Quercetin at 25 °C using a 600 MHz Varian INOVA nuclear magnetic resonance spectrometer in D₂O and D₂O:DMSO- d_6 (90:10, v/v), respectively.

2.4. Inclusion Complexation and Electrospinning. Clear and concentrated solutions of HP-β-CD and HP-γ-CD were prepared separately by dissolving each CD in 0.5 mL of distilled water to reach concentrations of 180% (w/v). Quercetin powder was then introduced into each of these CD solutions. Initially, solutions with different CD/Quercetin molar ratios were prepared to determine the highest molar ratio suitable for electrospinning. Consequently, two molar ratios, namely 4:1 and 8:1, were prepared for each CD, resulting in the preparation of the following samples: HP- β -CD/ Quercetin (4:1), HP- γ -CD/Quercetin (4:1), HP- β -CD/Quercetin (8:1), and HP- γ -CD/Quercetin (8:1). The solutions were gently mixed overnight at 37 °C to facilitate the formation of inclusion complexes between quercetin and CD. Subsequently, each of these CD/Quercetin solutions was allowed to be brought down to ambient temperature before electrospinning, eliminating any bubbles present in the solutions.

Electrospinning was carried out using a temperature- and humidity-controlled Spingenix SG100-CSS1000 device (Palo Alto, CA, USA). Each prepared solution was loaded into plastic syringes equipped with 27 G metal needles. A syringe pump, maintaining a flow rate of 0.5 mL/h, was used to push the solutions through the needles. Positioned at a distance of 12–15 cm from the needle tip, a grounded metal collector coated with aluminum foil was employed to collect the electrospun nanofibrous coatings. Using a high-voltage power supply, a constant voltage within the range of 18–21 kV was applied. The electrospinning process took place under ambient conditions with a temperature set at 20 °C and relative humidity maintained at 25%.

After the nanofibers were prepared and considering the results of phase solubility and through physicochemical, antibacterial, and antioxidant investigations, HP-γ-CD/Quercetin (8:1) was chosen as the optimum nanofibrous system. To further improve the biofunctionality of HP-γ-CD/Quercetin nanofibers, chitosan was added to the HP-γ-CD/Quercetin (8:1) system, thus preparing the Chitosan/HP-γ-CD/Quercetin (8:1) nanofibers. For this purpose, a 6% (w/v) chitosan solution was prepared in the water/acetic acid mixture (1/9 v/v). Consequently, the 200% (w/v) aqueous mixture of HP-γ-CD was prepared, which resulted in HP-γ-CD/Quercetin (8:1) inclusion complexation by adding quercetin. After 24 h of mixing, the chitosan and the inclusion complexation solutions were mixed with a 1 to 3 ratio (v/v), respectively, and stirred for 24 h at room temperature. To be used as the control system for biological properties, pristine Chitosan/HP-γ-CD nanofibers were fabricated by applying the same material concentrations and procedure, except without the addition of quercetin and the development of inclusion complexation. In this respect, similar to the Chitosan/HP-γ-CD/ Quercetin (8:1) solution, the 6% (w/v) chitosan solution in a water/ acetic acid mixture (1/9 v/v) and a 200% (w/v) aqueous mixture of HP- γ -CD were mixed with a ratio of 1 to 3 (v/v), respectively.

- **2.5.** Investigation of Solution Properties. Electrical conductivities of the electrospinning solutions were evaluated at ambient temperature using a conductivity meter (FiveEasy, Mettler Toledo, USA). In parallel, viscosity measurements of the solutions were conducted using a rheometer (AR 2000, TA Instruments, USA) with a 20 mm cone/plate accessory (CP 20-4 spindle type, 4°). The tests were executed across a shear rate span of 0.01–1000 s⁻¹ at a constant temperature of 22 °C.
- **2.6. Morphological Analysis.** Tescan MIRA3 scanning electron microscopy (SEM, Czech Republic) was employed to investigate the morphological characteristics of the nanofibers produced from HP- β -

CD/Quercetin (4:1), HP- γ -CD/Quercetin (4:1), HP- β -CD/Quercetin (8:1), HP- γ -CD/Quercetin (8:1), and Chitosan/HP- γ -CD/Quercetin (8:1). To prevent electrical charging complications, a Au/Pd coating was applied to the samples before the tests. The nanofibers were imaged by using SEM with a 12 kV accelerating voltage and a working distance of 10 mm. The nanofiber diameters were analyzed with ImageJ software by randomly choosing 100 nanofibers and subsequently calculating the average fiber diameter.

2.7. Determining the Loading Efficiency. The loading efficiency (%) of quercetin in nanofibrous samples was investigated by dissolving nanofibrous samples in dimethyl sulfoxide (DMSO) and measuring the quercetin concentrations by UV–vis spectroscopy using a quercetin calibration curve in DMSO. The tests were performed in triplicate, and the findings were stated as the mean ± standard deviation. The loading efficiency (LE) was measured by using the following formula:

$$LE (\%) = (C_e/C_t) \times 100$$

Here, C_e is the quercetin content in the nanofibrous sample, while C_t is the total amount of quercetin used to prepare the fibers. To further investigate the loading efficiency, determine the CD/Quercetin molar ratios in the nanofibers, and assess the chemical structure of quercetin through the whole process of dissolving and electrospinning, proton nuclear magnetic resonance (¹H NMR, Bruker AV500 equipped with an autosampler) analysis was also conducted. Quercetin and HP-β-CD/Quercetin (8:1), HP-γ-CD/Quercetin (8:1), and Chitosan/HPγ-CD/Quercetin (8:1) samples were dissolved in deuterated dimethyl sulfoxide (DMSO-d₆), and ¹H NMR spectra were collected with 16 scans per sample. Mestranova software was utilized to apply a baseline correction to the obtained spectra, and chemical shifts (δ, ppm) were precisely integrated. The molar ratios of CD/Quercetin nanofibrous samples were evaluated through the signal corresponding to the -CH₃ protons of CD, resonating at 1.03 ppm, and the protons associated with quercetin, which showed chemical shifts from 6.1 to

- **2.8. Differential Scanning Calorimetry (DSC) Analysis.** The thermal characteristics of quercetin and chitosan powders, as well as HP- β -CD/Quercetin (8:1), HP- γ -CD/Quercetin (8:1), and Chitosan/HP- γ -CD/Quercetin (8:1) nanofibers, were studied using a differential scanning calorimeter (DSC, Q2000, TA Instruments, USA). The samples were meticulously weighed and enclosed within Tzero aluminum pans to prepare them for the DSC evaluations. Subsequently, the samples underwent controlled heating, progressing from 0 to 275 °C at a heating rate of 10 °C/min while situated under a N₂ atmosphere.
- **2.9.** X-ray Diffraction (XRD) Analysis. X-ray diffraction (XRD) patterns were generated for quercetin and chitosan powders as well as HP- β -CD/Quercetin (8:1), HP- γ -CD/Quercetin (8:1), and Chitosan/HP- γ -CD/Quercetin (8:1) nanofibers using an X-ray diffractometer (XRD, Bruker D8 Advance ECO). Configuring the voltage and current to 40 kV and 25 mA, Cu–K α radiation was employed for the acquisition of XRD patterns, covering the 2 θ angle range from 5° to 30°.
- **2.10. Fourier Transform Infrared (FT-IR) Analysis.** The attenuated total reflectance Fourier transform infrared (ATR-FT-IR) spectra of quercetin and chitosan powders as well as HP- β -CD/Quercetin (8:1), HP- γ -CD/Quercetin (8:1), and Chitosan/HP- γ -CD/Quercetin (8:1) nanofibers were obtained using an ATR-FT-IR spectrometer (PerkinElmer, USA). These spectra were obtained across wavenumbers spanning from 4000 to 600 cm⁻¹ with a 4 cm⁻¹ resolution, averaging 64 scans per measurement.
- **2.11. Thermogravimetric (TGA) Analysis.** The thermogravimetric behaviors of quercetin and chitosan powders and the CD/Quercetin nanofibrous samples were explored through a thermogravimetric analyzer (TGA, Q500, TA Instruments, USA). In the course of the TGA assessments, a precise amount of each sample was deposited onto a platinum TGA pan and then subjected to gradual heating. The temperature ascended from room temperature to 700 °C at a controlled rate of 10 °C/min while operating through a $\rm N_2$ atmosphere.

2.12. Antioxidant Activity Assessment. To assess the antioxidant activity of the quercetin powder and CD/Quercetin nanofibrous webs, a 2,2-diphenyl-1-picrylhydrazyl (DPPH) radical scavenging assay was employed. For concentration-dependent antioxidant tests, to compare the antioxidant activity, certain amounts of quercetin and nanofibers with the same quercetin contents were dissolved in PBS (pH 7.2) and then filtered by a 0.45 μ m PTFE filter to remove the undissolved quercetin in the solutions. Next, the prepared solutions were solution blended 1:1 with the DPPH solution to reach quercetin concentrations of 125–1000 (μ g/mL) and then shaken in the dark for 1 h. The reduction in the DPPH absorption (at 517 nm) was assessed via UV—vis spectroscopy. All experiments were conducted in three replications, and the radical scavenging efficiency of quercetin/CD webs was computed by the following formula:

inhibition (%) =
$$((A_{\text{control}} - A_{\text{sample}})/A_{\text{control}}) \times 100$$

Accordingly, $A_{\rm control}$ shows the absorbance of the control DPPH solution, while $A_{\rm sample}$ shows the absorbance of the sample solution.

2.13. In Vitro Antibacterial Evaluation. The antibacterial efficacy of the nanofibrous samples against two bacterial strains, Gram-negative Escherichia coli (E. coli) and Gram-positive Staphylococcus aureus (S. aureus), was determined through a colony counting technique. To conduct this analysis, the bacterial species were cultured overnight in 5 mL of Luria-Bertani (LB) medium incubating at 37 °C with aeration at 200 rpm in the absence of antibiotics. Overnight cultures were subsequently subcultured at a 1:100 ratio in LB medium and grown at 37 °C and 200 rpm with aeration until the optical density (OD_{600}) reached 1, equivalent to 10^9 colony forming units per milliliter (CFU/mL). From this concentration, dilutions were made in 1 mL of LB medium to achieve a final concentration of 10⁷ CFU/mL. Next, 50 mg of each UV-sterilized web was dissolved in 1 mL of the bacterial solution. As part of the analysis, an untreated culture solution was defined as the negative control, while another sample was treated with the 20 µg/mL antibiotic streptomycin to act as the positive control. The samples were incubated at 37 °C for 24 h. Post-incubation samples were diluted in phosphate-buffered saline (PBS, pH 7.2), and 100 μ L of the diluted samples was spread on LB agar plates for enumeration. Plates were incubated at 37 °C overnight. The next day, by counting the colonies on each plate, the antimicrobial activity of each sample was determined in relation to the negative control.

2.14. Investigating the Cell Viability of Nanofibers. As the primary focus of this study was to develop a nanofibrous wound dressing to aid wound healing, the potential toxicity of the produced nanofibers on fibroblast cells (3T3) was assessed using indirect 3-(4,5-dimethylthiazol-2-yl)-2,5-diphenyl-2H-tetrazolium bromide (MTT) assay following the ISO 10993-5 standard test method.³⁵ A culture medium comprising Dulbecco's Modified Eagle Medium (DMEM), 10% fetal bovine serum (FBS) (Gibco, USA), 100 U/mL penicillin, and 100 µg/mL streptomycin was prepared for this purpose. Murine embryonic fibroblast cell line (3T3) was cultured in a 96-well plate, with each well containing 100 μL of the culture medium, seeded at a density of 10⁵ cells/well, and then incubated at 37 °C for 24 h. According to the ISO 10993-12 protocol, ³⁶ the asprepared nanofibers were extracted from 6 cm² (~50 mg) nanofibrous mats after undergoing sterilization with UV irradiation for 30 min, followed by immersion in 1 mL of culture medium at 37 °C for 24 h.

After seeding the cells in the wells, the medium was removed from the wells and replaced with the corresponding nanofibers' extracts, which were reincubated for another 24 h at the same condition. The control group received fresh culture medium under identical conditions. Subsequently, after 24 h, the medium was replaced with fresh medium, and then 20 μ L of 5 mg/mL MTT (TCI, USA) solution was added to each well and left to incubate for 4 h. Afterward, to dissolve the resulting formazan crystals, the medium was removed, and 100 μ L of dimethyl sulfoxide (DMSO) was added to each well and uniformly mixed on a plate shaker. Optical density readings were taken at 570 and 630 nm by using an ELISA reader, and the average of the values was calculated from six replicates. The

viability percentage was determined compared with the control sample.

2.15. Investigating the Anti-Inflammatory Activity. Inflammation plays a major role in wound healing, and a suitable wound dressing should regulate it. In this respect, the anti-inflammatory activity of the nanofibers was investigated against two kinds of cells capable of generating the anti-inflammatory response, such as macrophages and regenerative epidermal cells. For this investigation, we employed the fibroblast cell line 3T3 as regenerative epidermal cells and the human monocyte cell line THP-1, which was differentiated into macrophages by using 10 ng/mL PMA (phorbol 12-myristate 13-acetate). The anti-inflammatory response was interrogated by stimulating the cells with an inflammatory compound, followed by the addition of the nanofibers or control and evaluating the concentration of the standard inflammation markers IL-6 and NO secretion in the culture medium. To measure the IL-6 secretion, THP-1 cells were cultured in medium consisting of Roswell Park Memorial Institute (RPMI) (Gibco, USA) and 10% (v/v) FBS and placed in a 24-well plate (10^5 cells/mL, 1 mL/well). Then, 1 μ g/mL lipopolysaccharide (LPS) (Invitrogen, USA) was added to each well to induce the inflammatory response, and the cells were incubated at 37 °C for 24 h. The nanofibrous samples were extracted in the same medium with the previously mentioned method. After the incubation, the cell medium was disregarded and replaced with the nanofiber extracts with the fresh medium as the control. LPS (1 μ g/mL) was maintained by adding it back to the wells to continue the inflammation. The cells were incubated for 10 h at 37 °C, and the IL-6 concentration was calculated in supernatants by ELISA (Invitrogen, USA). The investigation was conducted in three replicates.

The inflammation in 3T3 cells was investigated by evaluating the NO secretion. In this regard, the cells were first cultured in a 24-well plate in RPMI and 10% (v/v) with 1 μ g/mL LPS to elicit inflammation (10^S cells/mL, 1 mL/well). After 24 h at 37 °C, the medium was replaced with nanofiber extract and incubated for 10 h at 37 °C. The supernatants were then removed from the wells, and the levels of NO were investigated using a Griess reagent kit (Invitrogen, USA) with three replications.

2.16. Coating the Cotton Nonwoven and the In Vitro Release. After the optimum conditions and nanofiber structures were determined, the nanofibers were coated on cotton nonwoven. Then, an in vitro release study was conducted to examine the release patterns of HP- β -CD/Quercetin (8:1), HP- γ -CD/Quercetin (8:1), and Chitosan/HP- γ -CD/Quercetin (8:1) nanofibrous samples, as well as cotton nonwoven substrates coated with these nanofibrous coatings. The self-standing nanofibrous webs, which weighed roughly 10 mg, were submerged in a 10 mL PBS solution with a pH of 7.4. These samples were then placed on an orbital shaker with a 200 rpm setting and maintained at 37 °C continuously.

In the case of nanofibrous-coated cotton samples, a 20 mg sample of each sample was added to a 10 mL PBS solution (pH 7.4) and shaken using an orbital shaker at 200 rpm and 37 °C. At predetermined intervals, 700 μ L samples were taken from each and replaced with the same amount of fresh PBS buffer. The concentration of each sample was measured at a wavelength of 321 nm using UV spectroscopy, considering the predetermined calibration curve. The experiment was carried out in triplicate (n=3), and the cumulative release of quercetin was obtained by monitoring the amount in each sample over the course of the experiment.

3. RESULTS AND DISCUSSION

3.1. Phase Solubility. Phase solubility analysis was employed to assess how inclusion complexation and the type of cyclodextrin (CD) affect the solubility of quercetin. Figure 2 depicts the phase solubility diagrams of the HP- β -CD/Quercetin and HP- γ -CD/Quercetin systems. These diagrams exhibited an A_L-type linear pattern, suggesting the formation of inclusion complexation with a 1:1 molar ratio. Inclusion complexation with both HP- γ -CD and HP- β -CD substantially

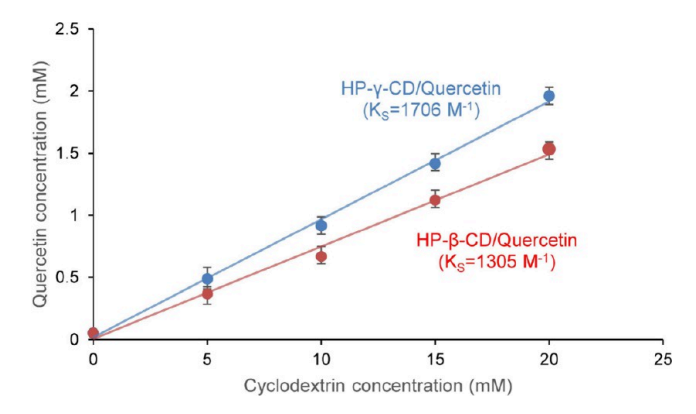


Figure 2. Phase solubility diagram of quercetin at varying concentrations of HP- β -CD and HP- γ -CD.

increased quercetin solubility, resulting in approximately 20-fold and 15-fold enhancements, respectively. These findings highlight the efficacy of this approach in improving quercetin solubility, a phenomenon well-documented in prior studies. 32,34

Accordingly, inclusion complexation with HP-γ-CD resulted in a better enhancement of quercetin solubility, which is attributed to the better size match between the quercetin molecule and the HP- γ -CD cavity. This size match is a crucial factor for the successful formation of inclusion complexes, encapsulation, and improved solubility. 10 In a related study on flavonoids, curcumin's solubility showed a similar trend, with greater improvement observed with HP-γ-CD due to its relatively larger molecular size.³⁷ Due to this significant improvement in quercetin solubility, the binding constants (K_S) for HP- β -CD and HP- γ -CD were calculated as 1305 and 1706 M⁻¹, respectively. This finding confirms the higher stability of HP-γ-CD/Quercetin inclusion complexation. The obtained data are in agreement with related studies on the inclusion complexation of quercetin with CDs. 19,38 Given that the limited solubility of quercetin is a primary challenge in harnessing its properties, these remarkable enhancements hold promise for its wide-ranging biomedical applications. Particularly, by a significant solubility increase of quercetin, nanofibers show the potential to act as a coating in the biofunctionalization of cotton for wound dressing applications.

3.2. Investigating the Formation of Inclusion Complexation by 2D-NMR. Rotating frame Overhauser effect spectroscopy (ROESY), a significant method in two-dimensional nuclear magnetic resonance (2D-NMR), is widely utilized for studying interactions involving cyclodextrins (CDs) due to its remarkable capability to discern interactions over distances of up to 5 Å. 39 In this investigation, we effectively employed the ROESY NMR technique to elucidate spatial host-guest interactions in solutions involving two distinct cyclodextrins, HP- β -CD and HP- γ -CD, along with quercetin, as shown in Figure 3. Examination of the ROESY spectrum for the HP-β-CD/Quercetin system revealed simultaneous proton resonances between the inner cavity protons (H_3 and H_5) of HP- β -CD and the aromatic protons of quercetin. Similarly, in the HP-γ-CD/Quercetin solution, the spectrum exhibited overlapping peaks of the inner cavity protons of HP- γ -CD (H₃ and H₅) and the aromatic protons of quercetin. Therefore, the 2D-NMR data clearly indicate the host—guest interactions and confirm the formation of inclusion

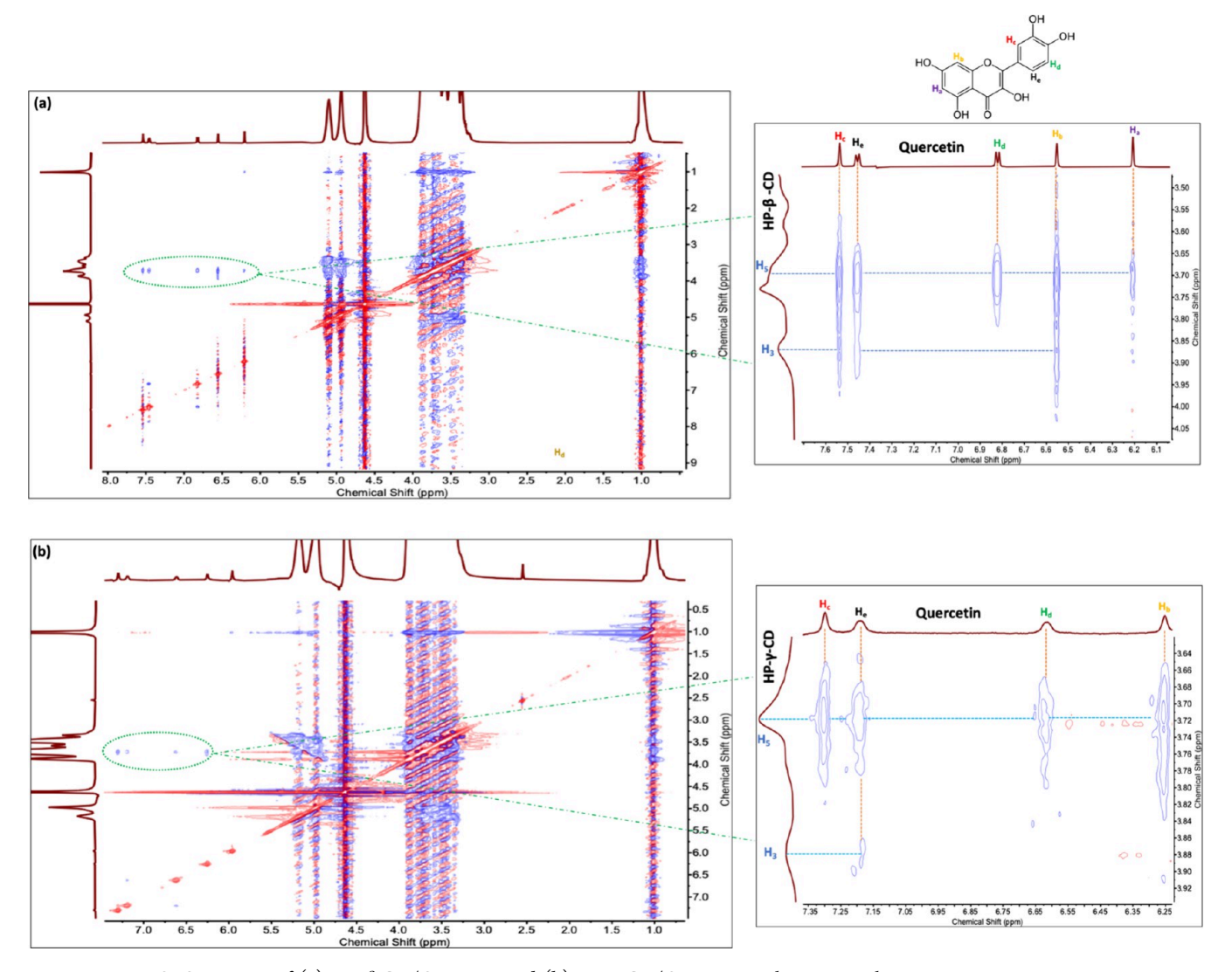


Figure 3. 2D ROESY spectra of (a) HP- β -CD/Quercetin and (b) HP- γ -CD/Quercetin inclusion complexations.

Table 1. Characteristics of the Solutions and Average Diameters of the Nanofibrous Samples

sample	CD concentration (g/100 mL) ^a	molar ratio (CD/Quercetin)	quercetin concentration $(w/w)^b$	chitosan concentration $(w/w)^b$	viscosity (Pa s)	conductivity (μS/cm)	average fiber diameter (nm)
HP-β-CD/Quercetin (4:1)	180%	4/1	5.0%	-	0.312	44.07	445 ± 95
HP-γ-CD/Quercetin (4:1)	180%	4/1	4.2%	-	0.776	9.47	665 ± 130
HP- β -CD/Quercetin (8:1)	180%	8/1	2.5%	-	1.182	48.91	675 ± 190
HP-γ-CD/Quercetin (8:1)	180%	8/1	2.1%	-	1.522	10.77	880 ± 250
Chitosan/HP- γ -CD/Quercetin (8:1)	150%	8/1	2.0%	1.0%	2.330	18.25	1110 ± 340

^aWith respect to the solvent (water). ^bWith respect to the total sample mass.

complexes between quercetin and both CDs (HP- β -CD, HP- γ -CD).

3.3. Electrospinning and Morphological Investigation of Nanofibers. To determine the optimum systems to prepare the CD/Quercetin nanofibers, inclusion complexations were prepared using different CD types (HP- β -CD and HP- γ -CD) and CD to quercetin molar ratios (CD/Quercetin; 4:1 and 8:1). The resulting complexes were electrospun, and an analysis of the nanofiber fabrication was conducted. Table 1 presents an overview of the solution properties, and Figure 4 displays the SEM images of the electrospun nanofibers.

Considering the SEM data, the solutions with the 4:1 molar ratio could not develop fine fibers, and they are beaded and defected. However, reducing the quercetin content to molar ratio of 8:1 resulted in the production of smooth and beaded nanofibers. The SEM images also show that the addition of chitosan to the HP- γ -CD/Quercetin nanofibers did not disturb the morphology of the nanofibers. Comparing solution properties revealed that a higher quercetin molar ratio significantly decreased the viscosity of the solution. This finding aligns with previous studies, indicating that an increased quercetin concentration can reduce the viscosity of

ACS Applied Bio Materials

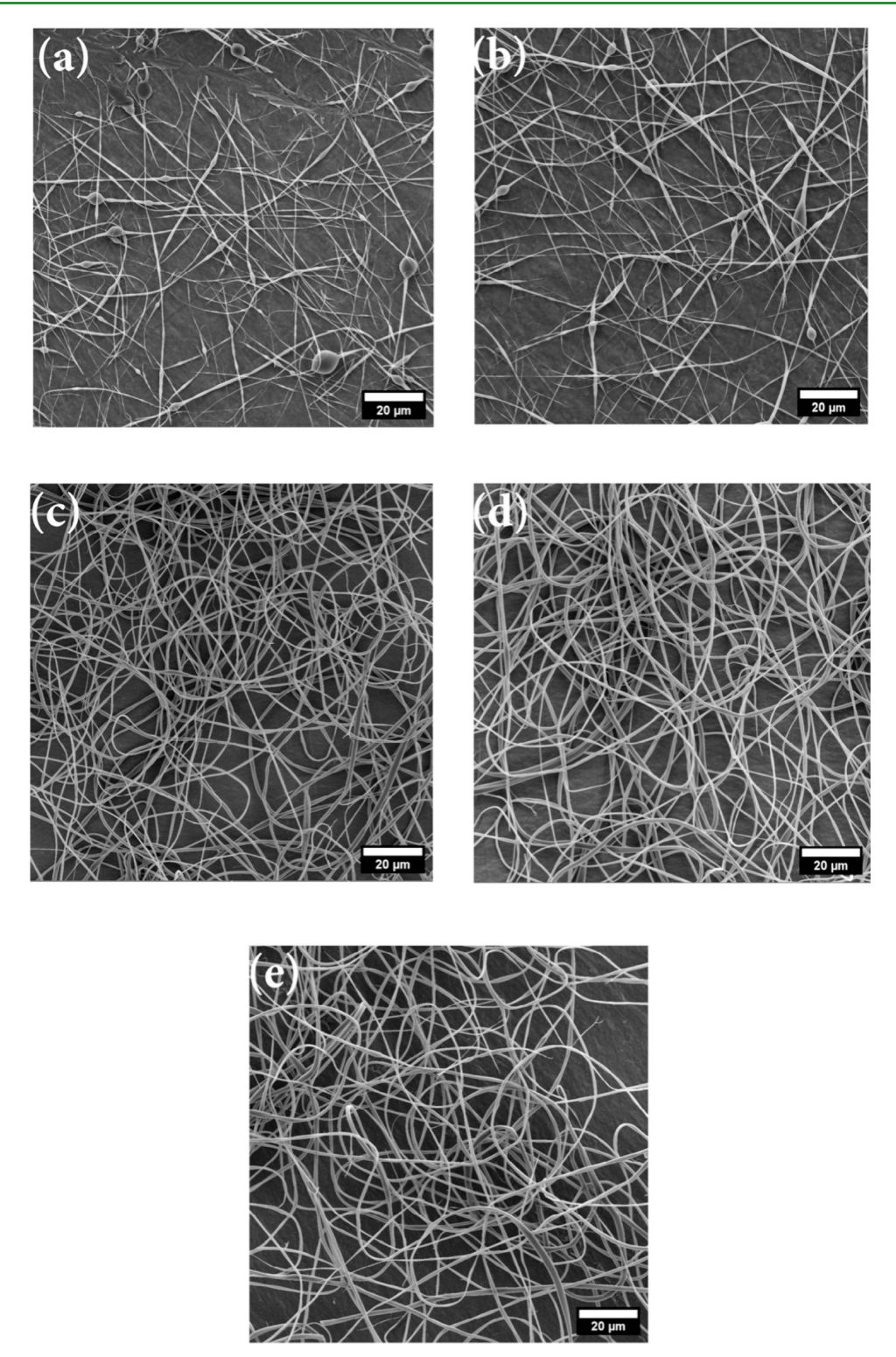


Figure 4. SEM images of nanofibers (a) HP- β -CD/Quercetin (4:1), (b) HP- γ -CD/Quercetin (4:1), (c) HP- β -CD/Quercetin (8:1), (d) HP- γ -CD/Quercetin (8:1), and (e) Chitosan/HP- γ -CD/Quercetin (8:1).

electrospun solutions.⁴⁰ This effect can be attributed to the plasticizing effect of quercetin. It was shown that quercetin can show a plasticizing effect.⁴¹ This plasticizing effect can make quercetin form hydrogen bonding with the hydroxyl groups of HP-CDs, leading to the disruption of CDs' intramolecular hydrogen bonding.⁴² This intramolecular hydrogen bonding is the main driving force for solution viscosity and electrospinning of polymer-free CDs. Thus, its disruption can result in

a lower solution viscosity. 43 This disruption of hydrogen bonding can be one of the reasons for the structural disturbance of the fibers in the 4:1 molar ratio.

Comparing the types of cyclodextrin, the average fiber diameter of HP- β -CD/Quercetin was smaller than that fabricated by HP- γ -CD consistent, with our previous findings. Tonsidering γ -CD's one additional glucopyranose unit, its solution exhibited higher viscosity, tesulting in larger

fiber diameters. ¹⁰ The results also showed that HP- β -CD/Quercetin nanofibers exhibited higher conductivity, which again can lead to the formation of smaller fibers.

Considering the phase solubility, HP-γ-CD formed a more favorable inclusion complexation with quercetin, resulting in the optimum nanofibrous system. Thus, to further improve the antibacterial properties of the nanofibers, chitosan was incorporated into HP-γ-CD/Quercetin (8:1) fibers. Investigating the solution properties of Chitosan/HP-γ-CD/Quercetin (8:1) revealed an increase in viscosity attributed to chitosan's structural composition, characterized by long chains of *N*-acetylglucosamine and glucosamine, along with a positive charge. This positive charge also resulted in a slightly higher solution conductivity; however, due to the significant increase in viscosity, the fiber diameter increased by the addition of chitosan.

Overall, the solution properties and SEM results highlight the significant influence of the molar ratio in the inclusion complexation of quercetin with HP- β -CD and HP- γ -CD on the nanofiber fabrication process. The 4:1 molar ratio resulted in a defective CD/Quercetin fiber morphology, while the 8:1 CD/Quercetin samples exhibited superior productivity, yielding a self-standing nanofibrous web with enhanced uniformity, making it the preferred choice for the electrospinning process. Moreover, the selection of CD type also plays a role in determining fiber size, where HP- β -CD produced thinner fibers than HP- γ -CD, attributed to the structural aspects of the cyclodextrins. The incorporation of chitosan in the CD/Quercetin system did not disturb the fiber structure, enabling benefit from its biological properties.

3.4. Loading Efficiency. The loading efficiency of quercetin in the fibers was calculated by dissolving the nanofibers in DMSO and comparing the quercetin content to the initial amount. Accordingly, the loading efficiencies were almost 100% for HP-γ-CD/Quercetin (8:1) and Chitosan/HP- γ -CD/Quercetin (8:1). The loading efficiency for HP- β -CD/ Quercetin (8:1) was slightly lower, at about 96%. This is attributed to the more stable complexation of quercetin and HP-γ-CD due to the better size match, as indicated by the phase solubility. The slightly lower encapsulation efficiency of $HP-\beta$ -CD indicates the possibility of noncapsulated quercetin occurring in HP- β -CD/Quercetin (8:1) nanofibers. The similarity between the loading efficiency of HP-γ-CD/ Quercetin (8:1) and that of Chitosan/HP-γ-CD/Quercetin (8:1) implies that the addition of chitosan did not disturb either the inclusion complexation or the electrospinning process. Overall, the obtained data show the near-complete encapsulation of quercetin into the nanofibers through inclusion complexation by electrospinning.

For further investigation of the loading efficiency and the determination of CD/Quercetin molar ratios in the fibers, as well as the chemical structure of quercetin, 1H NMR was performed. Figure 5 shows the 1H NMR spectra of quercetin and the prepared nanofibers. Previous studies showed that CDs show a unique identification peak at 1.03 ppm ($-CH_3$). The identification peaks of quercetin are between 6.1 and 7.7 ppm, which are attributed to the two rings of the quercetin molecule (as shown in Figure 5). Considering the difference between the integration of quercetin and CD peaks, the CD/Quercetin molar ratio in HP- β -CD/Quercetin (8:1), HP- γ -CD/Quercetin (8:1), and Chitosan/HP- γ -CD/Quercetin (8:1) nanofibers was found to be 7.46/1, 7.81/1, and 7.74/1, respectively. Therefore, the encapsulation efficiencies for

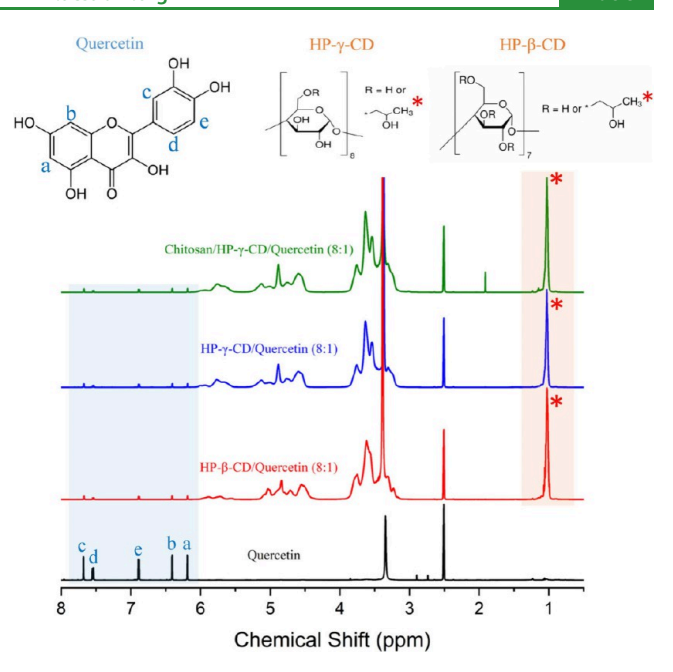


Figure 5. ¹H NMR spectra of quercetin powder as well as HP- β -CD/Quercetin (8:1), HP- γ -CD/Quercetin (8:1), and Chitosan/HP- γ -CD/Quercetin (8:1) nanofibers.

HP- β -CD/Quercetin (8:1), HP- γ -CD/Quercetin (8:1), and Chitosan/HP-γ-CD/Quercetin (8:1) were measured as 93%, 98%, and 97%, respectively. The results are in line with the loading efficiency measurements, showing a slightly higher efficiency in the case of HP-γ-CD due to the more stable inclusion complexation. The incorporation of chitosan within the fibers resulted in the occurrence of a new signal peak at 1.9 ppm in the Chitosan/HP-γ-CD/Quercetin (8:1) sample, corresponding to NH[CO]CH₃.46 The addition of chitosan also did not disturb the inclusion complexation between quercetin and HP- γ -CD, as the loading efficiency is about the same without the presence of chitosan. Moreover, as indicated by the NMR data, a consistent pattern of quercetin's characteristic peaks was observed in all nanofibrous samples, demonstrating the protection of quercetin's chemical structure through the fabrication processes. The NMR results confirm the successful loading of quercetin within the HP-β-CD, HP-γ-CD, and Chitosan/HP-γ-CD nanofibers and illustrate the chemical structural integrity of encapsulated quercetin in the nanofibers.

3.5. DSC Analysis. Considering the crystalline nature of quercetin and the amorphous structure of CDs, the use of DSC analysis to assess the crystallinity offers valuable insights into the inclusion complexation of quercetin within the CD cavities. The DSC results are presented in Figure 6a. As shown before, the melting point of quercetin is approximately 320 °C, surpassing the maximum analysis temperature of 270 °C, in which CDs begin to degrade and was chosen as the maximum analysis temperature.³² However, quercetin shows a broadened endothermic peak at 135 °C, representing the structural change and transformation of the molecules hydrated in the anhydrous form.⁴⁷ Moreover, modified cyclodextrins such as HP- β -CD and HP- γ -CD, being amorphous materials, do not have any melting peaks but show a broad endothermic curve between 60 and 140 °C due to the dehydration of CDs.³ Chitosan also shows a broad endothermic curve between 100 and 150 °C due to water evaporation.⁴⁸

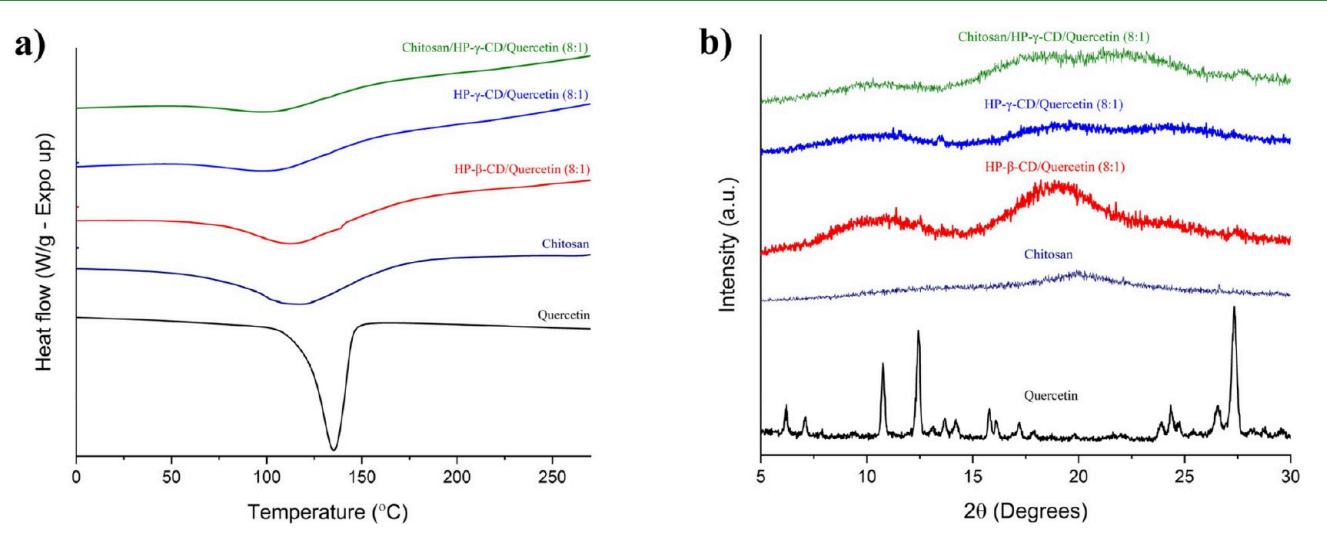


Figure 6. Crystal structural examination. (a) DSC thermograms and (b) XRD graphs of quercetin and chitosan powders as well as HP- β -CD/Quercetin (8:1), HP- γ -CD/Quercetin (8:1), and Chitosan/HP- γ -CD/Quercetin (8:1) nanofibers.

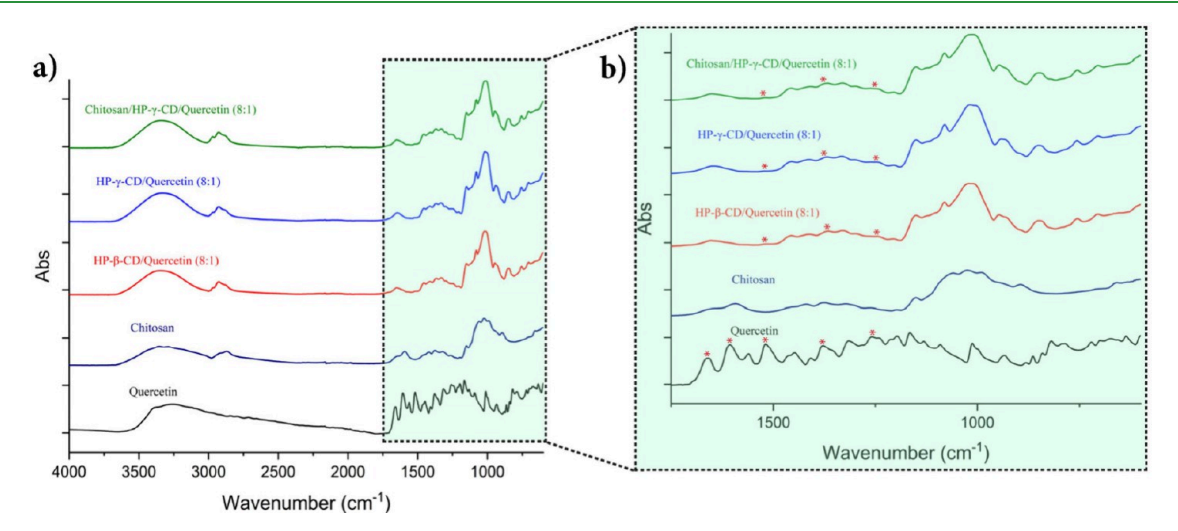


Figure 7. Chemical structure analysis. (a) The full and (b) the expanded range FT-IR spectra of the quercetin and chitosan powders as well as HP- β -CD/Quercetin (8:1), HP- γ -CD/Quercetin (8:1), and Chitosan/HP- γ -CD/Quercetin (8:1) nanofibers.

Considering the DSC curves of the nanofibrous samples, a broad peak at 90 °C is presented, corresponding to the dehydration process of CDs. Accordingly, the DSC graph of HP- β -CD/Quercetin (8:1) shows a slight peak at 135 °C, which is attributed to the quercetin structural change. This peak can indicate a possible incomplete complexation of quercetin with HP- β -CD. In contrast, this peak is not clear in the HP- γ -CD/Quercetin samples. This observation suggests a better complexation potential between HP- γ -CD and quercetin, a finding consistent with the results of the phase solubility analysis.

3.6. XRD Analysis. For a more comprehensive investigation of the crystalline structure of quercetin and nanofibers and to provide a perspective on the inclusion complexation, XRD analysis was performed. The XRD patterns of materials and nanofibrous samples are presented in Figure 6b. As a known crystalline compound, quercetin exhibits distinct diffraction peaks at 10.8°, 12.4°, 15.8°, 16.3°, 23.85°, 24.34°, 26.58°, and its sharp peak at 27.3°. As HP-CDs are amorphous, through inclusion complexation the quercetin molecules should be separated within the CD cavity and cannot form crystals. Therefore, the crystalline peaks would disappear in the

XRD patterns of CD/Quercetin inclusion complex systems. 30,34

Considering the amorphous nature of the nanofibrous samples, only subtle peaks at 12.4° and 27.3° are seen in the XRD patterns of the CD/Quercetin nanofibrous samples, revealing that quercetin molecules are mostly in an inclusion complexation state within the CD cavities and that there was a presence of a very small amount of uncomplexed quercetin in the CD/Quercetin nanofibrous samples. The quercetin crystalline peaks at 12.4° and 27.3° are a bit slightly less obvious in HP-γ-CD/Quercetin compared to HP-β-CD/ Quercetin nanofibers, suggesting that HP-γ-CD has a higher complexation efficiency with quercetin, showing agreement of the XRD data with the DSC and phase solubility findings. Similar to the DSC results, due to the more stable inclusion complexation and better size match, the inclusion complexation of quercetin with HP-γ-CD resulted in a much smaller amount of quercetin crystals. This is due to the prevention of quercetin molecules from forming crystals in the CD cavity. Moreover, the intensity of the quercetin crystalline peaks is the lowest in the Chitosan/HP-γ-CD/Quercetin nanofibers, which aligns with their lower quercetin content.

Article

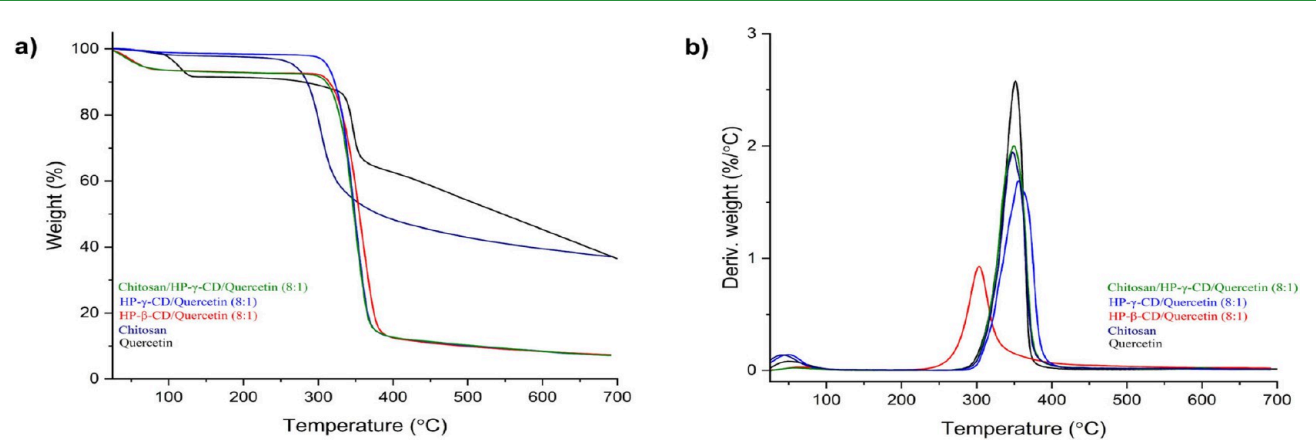


Figure 8. Thermal degradation profile. (a) TGA thermograms and (b) the derivative graphs (DTG) of quercetin and chitosan powders as well as $HP-\beta$ -CD/Quercetin (8:1), $HP-\gamma$ -CD/Quercetin (8:1), and Chitosan/ $HP-\gamma$ -CD/Quercetin (8:1) nanofibers

3.7. FT-IR Analysis. FT-IR analysis can reveal the details of the chemical interactions between the CD cavity and the guest molecule. Inclusion complexation can lead to the vanishing of the characteristic peaks, the reduction of peak intensity, or shifts in peak positions. 34,37 Figure 7 shows the FT-IR spectra of quercetin, chitosan, and nanofibrous samples. For the nanofibrous samples, the main characteristic peaks of HP- β -CD and HP- γ -CD around 1019, 1080, and 1150 cm⁻¹ are attributed to coupled C-C/C-O and antisymmetric C-O-C glycosidic bridge stretching.³⁷ The peaks at 3000-3600, 2928, 1651, and 1367 cm⁻¹ are assigned to O-H stretching, C-H stretching, O-H bending, and -CH3 bending of cyclodextrin. ¹⁰ For quercetin, the main characterization peaks are at around 3200-3600 cm⁻¹, attributed to O-H vibration; 1662 cm⁻¹, assigned to carbonyl stretching vibration of C=O; 1606 cm⁻¹, due to C=C stretching; and 1518 cm⁻¹, related to the aromatic group. The ones at 1382 and 1254 cm⁻¹ are due to C-OH and C-O-C vibration, respectively.^{32,34} The FT-IR spectra of chitosan show characterization bands at 1654 and 1592 cm⁻¹, attributed to the C=O stretching vibration of amid I and the N-H bending of amid II, respectively.⁴⁹ The broad band at 3344 cm⁻¹ is also assigned to intermolecular hydrogen bonding between N-H and O-H.50 The peaks at 1425 and 1372 cm⁻¹ are attributed to -CH₃ deformation, while the one at 1150 cm⁻¹ once again is due to the C-O-C glycosidic bridge of the saccharide structure.⁵

As is evident in the FT-IR spectra, there is no difference between the nanofibers fabricated with HP- β -CD and HP- γ -CD. Accordingly, most characterization peaks of quercetin are masked in the nanofibers, indicating the inclusion complexation of the samples. However, the C-OH and C-O-C vibration peaks of quercetin showed themselves as small peaks shifted from 1382 and 1254 cm⁻¹ to 1366 and 1248 cm⁻¹, respectively. Besides, the peak at 1518 cm⁻¹, related to the aromatic group, showed itself as a tiny peak in the nanofibers shifted to 1514 cm⁻¹. Overall, the FT-IR data indicate the inclusion complexation state of quercetin with HP-β-CD and HP-γ-CD in the nanofibers. Considering the very small amount of chitosan (1% w/w) and the similar saccharide structure of CD and chitosan, the characteristic peaks of chitosan are masked in Chitosan/HP-γ-CD/Quercetin nanofibers. The similar patterns between HP-γ-CD/Quercetin nanofibers and Chitosan/HP-γ-CD/Quercetin nanofibers confirm that chitosan did not affect the chemical nature of the nanofibers.

3.8. TGA Analysis. The thermal properties of quercetin, chitosan, and the as-prepared nanofibers were assessed for further investigation of inclusion complexation. The TGA analysis along with the corresponding DTG curves are presented in Figure 8. Accordingly, quercetin showed a slight weight loss (7%) between 92 and 130 °C, followed by the main degradation peak between 328 and 365 °C. This result, in accordance with other studies, indicates the thermal stability of quercetin, which shows a degradation peak higher than those of CDs.³⁴ Considering the DSC diagram of quercetin, the lack of degradation at 135 °C corroborates the structural change of quercetin in this DSC peak. Chitosan also showed the main degradation between 260 to 370 °C, followed by a slight degradation step after 370 °C.

Article

Regardless of the type of CD, the nanofibrous samples showed similar degradation behavior between 300 and 400 °C, which is associated with CD degradation. Anofibers showed an initial weight loss of about 6% until 100 °C, corresponding to water removal from the CD. The CD nanofibers followed the same trends as the pristine CD. It was shown that pristine HP- β -CD and HP- γ -CD nanofibers show the same TGA pattern, exhibiting degradation peaks from 280 and 430 °C. Thus, the thermal degradation step of quercetin shifted to a higher temperature due to the inclusion complexation. Furthermore, Chitosan/HP- γ -CD/Quercetin showed about 1% weight loss between 260 (the beginning of the chitosan degradation) due to chitosan degradation.

3.9. Antioxidant Activity. Effective management of oxidative stress plays a pivotal role in expediting wound healing and regulating inflammation to prevent scar formation. Thus, functionalization of the cotton surface with an active antioxidant coating can facilitate the woundhealing process. Quercetin, renowned for its viable antioxidant and anti-inflammatory activities, owes its efficiencies to its ability to neutralize reactive oxygen species. Additionally, it enhances the body's antioxidant capacity by modulating enzymatic activity and signal transduction pathways. These features have led quercetin to be extensively used as an antioxidant agent in wound dressing applications.

One of the primary challenges associated with utilizing quercetin in wound dressings is its limited solubility. In this study, we addressed this limitation by enhancing the solubility of quercetin through inclusion complexation with HP- β -CD and HP- γ -CD. Figure 9 illustrates the antioxidant activity of

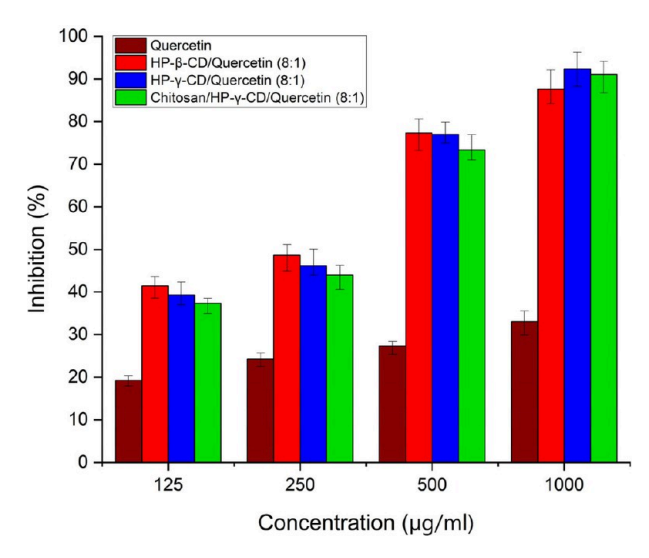


Figure 9. Antioxidant activity of quercetin powders as well as HP- β -CD/Quercetin (8:1), HP- γ -CD/Quercetin (8:1), and Chitosan/HP- γ -CD/Quercetin (8:1) nanofibers. The nanofibers and quercetin were dissolved to reach quercetin concentrations of 125–1000 (μ g/mL).

different concentrations of the nanofibrous webs and quercetin. As observed, the poor solubility of quercetin in its powdered form resulted in the loss of most of the powder during filtration, thereby limiting its antioxidant activity. In contrast, all the nanofibrous samples demonstrated significant

potential in scavenging DPPH radicals, achieving approximately 90% inhibition. At lower concentrations, the HP-β-CD/Quercetin (8:1) nanofiber sample exhibited higher activity compared to the HP-γ-CD/Quercetin (8:1) nanofibers. This discrepancy can be attributed to the higher quercetin concentration (2.5% w/w) in HP- β -CD/Quercetin (8:1) relative to HP-γ-CD/Quercetin (8:1) (2.1% w/w) and Chitosan/HP- γ -CD/Quercetin (8:1) (2% w/w) samples. However, at the highest concentration, the antioxidant activity of the HP- γ -CD/Quercetin (8:1) sample surpassed that of the HP- β -CD/Quercetin (8:1) sample. This trend can be attributed to HP-γ-CD's superior ability to enhance quercetin solubility, a fact confirmed by the phase solubility test. In fact, at the highest concentration, the antioxidant activity of the HP- γ -CD/Quercetin (8:1) sample (~92%) was higher than that of the HP- β -CD/Quercetin (8:1) sample (~88%), as quercetin solubility was enhanced, confirmed by the phase solubility test. These results, which align with our group's previous research, 30,34 showed that upon improving the solubility of quercetin, the fibers possessed strong antioxidant activities. The addition of chitosan led to a very slight decrease in the antioxidant activity (~91%), as it can reduce the weight concentration of quercetin in the nanofibers. Comprehensively, the results showed the ability of the CD/Quercetin nanofibers to provide antioxidant activity upon coating on cotton. This antioxidant activity, combined with quercetin's established anti-inflammatory and cell proliferation properties,⁵⁵ holds

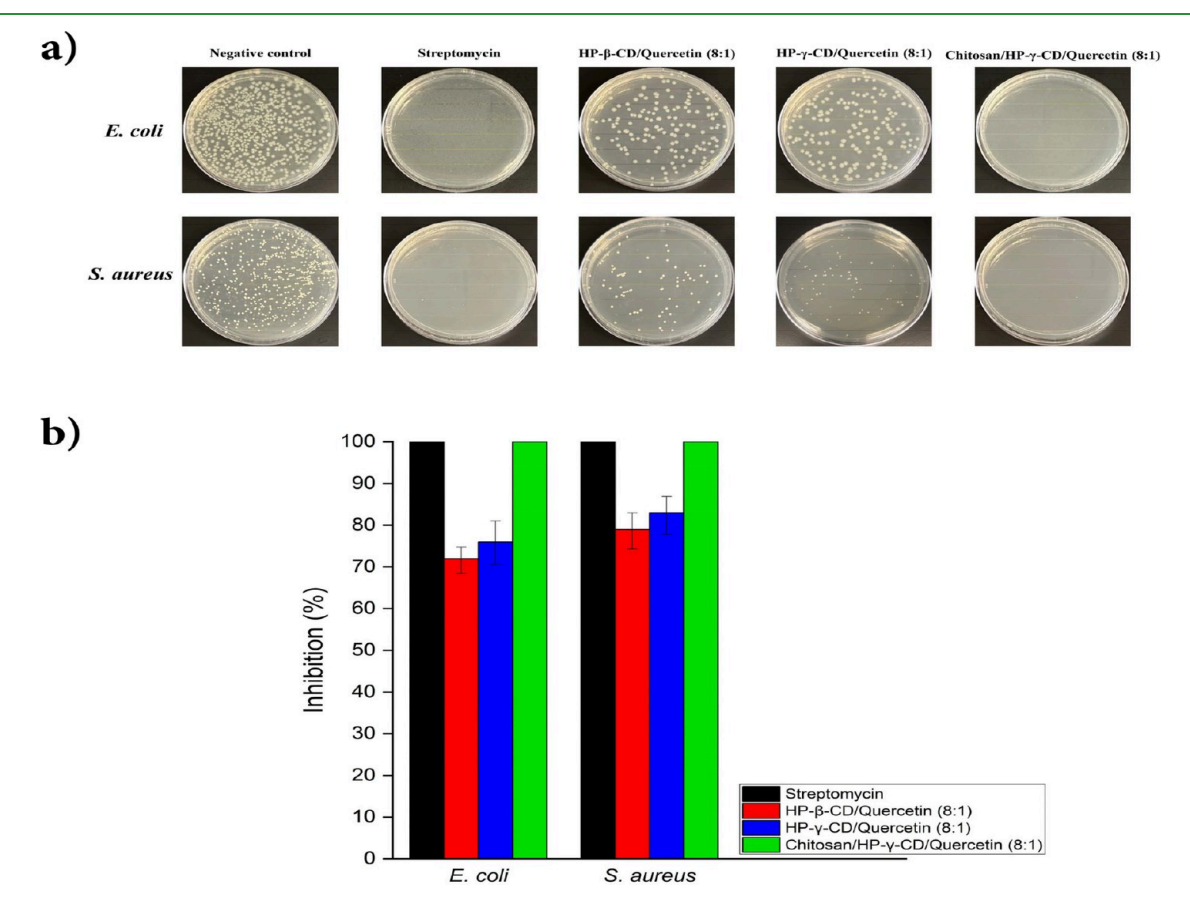


Figure 10. Antibacterial measurement by colony counting. (a) Photos of the formation of bacterial colonies. (b) Growth inhibition percentage of streptomycin as the positive control as well as HP- β -CD/Quercetin (8:1), HP- γ -CD/Quercetin (8:1), and Chitosan/HP- γ -CD/Quercetin (8:1) nanofibers against *E. coli* and *S. aureus*.

promise for enhancing wound healing and minimizing scar formation.

3.10. Antibacterial Activity. Preventing and controlling infection can play a pivotal role in achieving a defectless wound-healing process. Infections can induce an immune response, which can result in excessive inflammations, impairing the healing process, and scar formation. Besides, these infections can become systemic, which results in major complications. Quercetin is known for its moderate antibacterial activities.⁵⁶ Its activity is attributed to the interaction of its hydroxyl group with the bacterial cell membrane.⁵⁷ Thus, other than inclusion complexation, chitosan was incorporated into the optimum sample to increase the antibacterial activity. Chitosan derives its antibacterial efficacy from its positive charge, allowing it to interact with negatively charged bacterial cell walls and selectively bind to trace metal elements. This interaction hinders toxin production and inhibits microbial growth.50

The antibacterial activities of the nanofibrous samples were investigated against E. coli and S. aureus by colony counting methods. These bacteria are two of the main Gram-negative and Gram-positive bacteria associated with infections. Figure 10a illustrates the colonies formed and the antibacterial activity of the nanofibrous samples. The negative control exhibited no antibacterial activity, while the positive control effectively eradicated all bacteria. Figure 10b shows the inhibition percentages of samples against these bacterial species. Accordingly, HP-β-CD/Quercetin (8:1) and HP-γ-CD/ Quercetin (8:1) resulted in partial elimination of the bacteria as they respectively showed about 72% and 76% antibacterial activities against E. coli and 79% and 83% antibacterial activities against S. aureus. This observation is consistent with the fact that quercetin tends to be more effective against Gram-positive bacteria. The slightly higher activity of HP- γ -CD/Quercetin (8:1) against bacterial species is attributed to the notable enhancement of the quercetin solubility.

The presence of chitosan in the Chitosan/HP- γ -CD/Quercetin (8:1) nanofibers led to a remarkable improvement in antibacterial activity, completely eliminating the bacteria. Notably, this significant enhancement was achieved with a relatively low concentration of chitosan (1% w/w) in the nanofibers. Furthermore, the synergistic interaction of quercetin and chitosan contributed to the enhanced antibacterial properties of the nanofibers.

In brief, the inclusion complexation of quercetin with CDs resulted in favorable antibacterial activity within the nanofibers, a property further enhanced by the introduction of chitosan. The Chitosan/HP- γ -CD/Quercetin (8:1) sample exhibited outstanding antibacterial activity, which, combined with its effective antioxidant and other therapeutic properties, positions these nanofibers as a potent coating for enhancing the functionality of cotton nonwoven materials in wound dressing applications. Using all-natural-based materials without the use of synthetic antibiotics, this approach can further pave the way in addressing the challenge of synthetic antibiotic resistance.

3.11. Cell Viability. Besides suitable antibacterial activity, a functional wound dressing should not harm the cells and must provide an environment for their growth. In this respect, the toxicity of the as-prepared fibers was detected against the 3T3 fibroblast cell line, as shown in Figure 11. Accordingly, all the nanofibrous samples showed minimal toxicity against the cell line, providing almost complete viability. Considering the use of all-natural materials for the fabrication of nanofibers, these

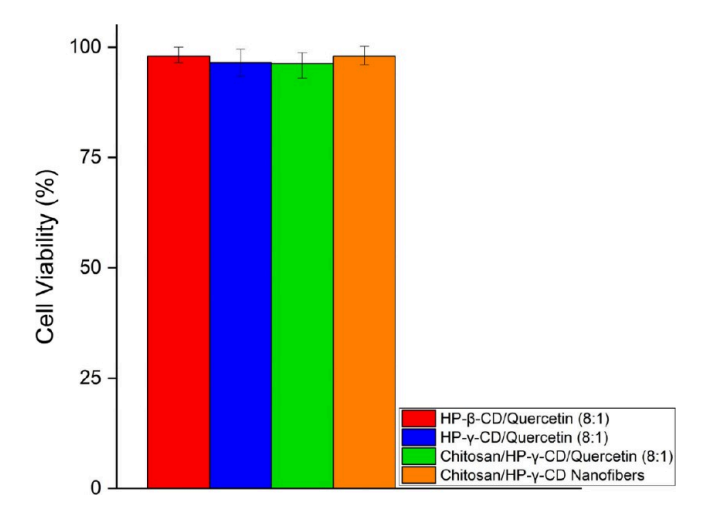
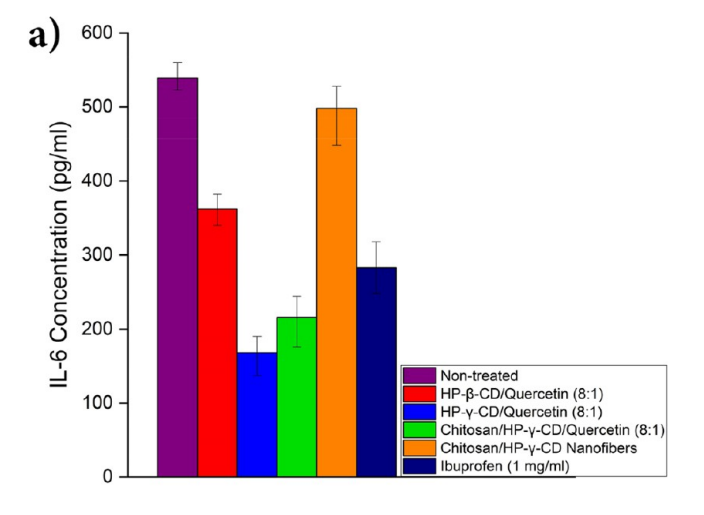


Figure 11. Cytotoxicity measurement. The viability of the fibroblast (3T3) cell line against HP- β -CD/Quercetin (8:1), HP- γ -CD/Quercetin (8:1), and Chitosan/HP- γ -CD/Quercetin (8:1) as well as pristine Chitosan/HP- γ -CD nanofibers after 24 h.

results were expected. Quercetin as the main bioactive compound has shown to be well-tolerated by cells due to its natural origin. Cyclodextrin and chitosan also being originated from natural materials do not harm the cells. The results confirm that this nanofibrous coating, despite its potent antibacterial activity, would not harm fibroblast cells, which is beneficial in aiding wound healing.

3.12. Anti-Inflammatory Activity. Inflammation is a vital part of wound healing, and its management can lead to its promotion. Immoderate inflammation can disrupt tissue regeneration and hinder wound healing.⁶¹ Both immune and regenerative cells can play roles in inducing an inflammatory response. Macrophages play a critical role in wound-healing inflammation, secreting various cytokines and growth factors to regulate immune response.⁶² Interleukin-6 (IL-6) is released by macrophages in response to an injury or specific microbial molecules inducing fever and production of acute-phase proteins from the liver. 63 The upregulation and prolonged expression of this pro-inflammatory cytokine may result in excessive inflammation and scar formation.⁶⁴ As an antiinflammatory bioactive, quercetin decreases the secretion of IL-6 by interfering with the response of cells to proinflammatory factors and decreasing the susceptibility of the immune cells to pro-inflammatory factors (such as LPS).⁶⁵

The anti-inflammatory activity of CD/Quercetin nanofibers was first investigated by measuring the concentration of IL-6 secreted by macrophages (THP-1) in culture supernatants. As Figure 12a shows, the untreated cells secreted 539 pg/mL IL-6, showing the magnitude of inflammation of the cells due to LPS stimulation. These levels of IL-6 were notably decreased by the addition of nanofibrous extracts. Accordingly, HP-β-CD/ Quercetin (8:1) and HP-γ-CD/Quercetin (8:1) showed about a 70% and 33% decrease in IL-6 concentration. The significant difference between HP-β-CD/Quercetin and HP-γ-CD/Quercetin nanofibers comes from the better inclusion complexation of quercetin with HP-γ-CD, as revealed from our results in this study. The Chitosan/HP-γ-CD/Quercetin (8:1) sample showed a small difference compared to the HP-γ-CD/ Quercetin (8:1) sample without chitosan, as there is a difference in quercetin amount in these samples. The pristine Chitosan/HP-γ-CD nanofibers without the presence of



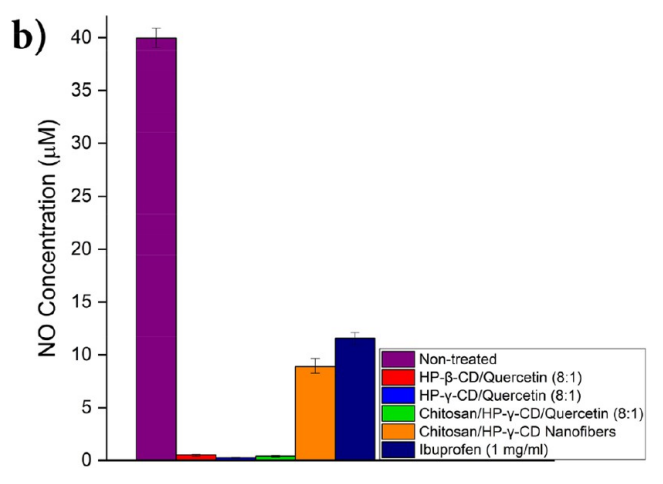


Figure 12. Measurement of anti-inflammatory activity by ELISA. Expression of (a) IL-6 and (b) NO against HP- β -CD/Quercetin (8:1), HP- γ -CD/Quercetin (8:1), Chitosan/HP- γ -CD/Quercetin (8:1), and pristine Chitosan/HP- γ -CD nanofibers as well as ibuprofen secreted from (a) macrophages (THP-1) and (b) fibroblasts (3T3).

quercetin also showed a slight anti-inflammatory response, as there are various contradicting studies about chitosan activity in reducing IL-6. Ibuprofen was used as a nonsteroidal anti-inflammatory drug for comparison. Accordingly, the use of 1 mg/mL ibuprofen led to a $\sim\!51\%$ reduction in IL-6 concentration, which was lower than the HP- γ -CD/Quercetin nanofibrous samples, showing their potency as anti-inflammatory agents.

Fibroblasts play a huge role in skin regeneration and wound healing. Excessive production of pro-inflammatory mediators by fibroblasts, along with persistent inflammation, is one of the main reasons for fibroblast dysfunction leading to chronic wounds, fibrosis, and scars. Nitric oxide (NO) also acts as a signaling pathway, playing a key role in the pathogenesis of inflammation. Thus, the secretion of NO in fibroblasts (3T3) was investigated for the next step and is illustrated in Figure 12b. As evident, all the quercetin-loaded nanofibrous samples almost completely diminished the NO concentration in the cell supernatants. The inclusion complexation between CD and quercetin led to this complete NO reduction, as it was shown that quercetin can inhibit the secretion of NO. It was suggested that the low solubility of quercetin is the main obstacle in exploiting its anti-inflammatory activity, while

increasing the water solubility by encapsulating quercetin in nanoparticles resulted in the downregulation of IL-6 and NO secretion. Pristine Chitosan/HP- γ -CD nanofibers also reduced the NO concentration by about 78%, which can be due to the existence of chitosan. It was shown that chitosan in certain molecular weights can show an anti-inflammatory response by reducing NO secretion.

These comprehensive anti-inflammatory activities are particularly useful for the treatment of chronic wounds, as they usually remain in the inflammatory phase for a long time. By regulating the inflammation caused by both immune and regenerative cells, in addition to their suitable antioxidant activity, the fabricated HP- β -CD/Quercetin (8:1), HP- γ -CD/Quercetin (8:1), and Chitosan/HP- γ -CD/Quercetin (8:1) can expedite the wound-healing process and decrease the chance of scar formation.

3.13. Nanofibrous Coating on Cotton Nonwoven and Quercetin Release. This study aimed to produce a cotton-based wound dressing by coating cotton with a biofunctional electrospun coating, in which the cotton can act as an outer layer. Using a flavonoid can provide wound-healing and antibacterial properties to the wound dressing, and inclusion complexation can improve the solubility and bioavailability of the flavonoid. In this respect, the HP- β -CD/Quercetin (8:1), HP- γ -CD/Quercetin (8:1), and Chitosan/HP- γ -CD/Quercetin (8:1) nanofibers were coated on cotton nonwoven, as depicted in Figure 13a.

The release profiles of the coated cotton and the freestanding nanofibers were measured and are presented in Figure 13b. Accordingly, the nanofibers showed a fast-dissolving behavior, as they are not cross-linked, and the fast dissolution of the nanofibers resulted in the immediate release of quercetin. All the nanofibers released quercetin within the first 3 min, confirming the fast-dissolving behavior of all the samples. As evident, HP-γ-CD nanofibers resulted in a higher cumulative release, confirming the loading efficiency and phase solubility results indicative of the more suitable complexation with quercetin. Besides, the coated cotton showed the same profiles as the free-standing nanofibrous webs since there is no chemical cross-linking between the cotton and the nanofiber coatings. The incorporation of chitosan in the nanofibers did not hinder the quercetin release, confirming that chitosan in this low concentration did not change the inclusion complexation and nanofiber structure. Applying this fast-dissolving nanofibrous coating on cotton nonwoven has the potential to release a high amount of quercetin to the wound site, which can facilitate healing and prevent infection. Coated cotton with increased quercetin solubility, providing its swift release, can hold promise to act as a suitable wound dressing for highly infected wounds such as diabetic ulcers.

4. CONCLUSION

In wound dressing applications, substrate choice is crucial, with cotton being a preferred choice over synthetic materials due to its biocompatibility and favorable physical properties. In this study, quercetin was employed to induce antioxidant and antibacterial activities. Overcoming the hurdle of quercetin's limited solubility in biomedical applications, a biofunctional wound dressing was created by enhancing quercetin solubility through inclusion complexation with CDs and coating CD/ Quercetin nanofibers onto cotton. Phase solubility results indicated a remarkable 20-fold increase in quercetin water-solubility through inclusion complexation, with HP- γ -CD

ACS Applied Bio Materials www.acsabm.org Article

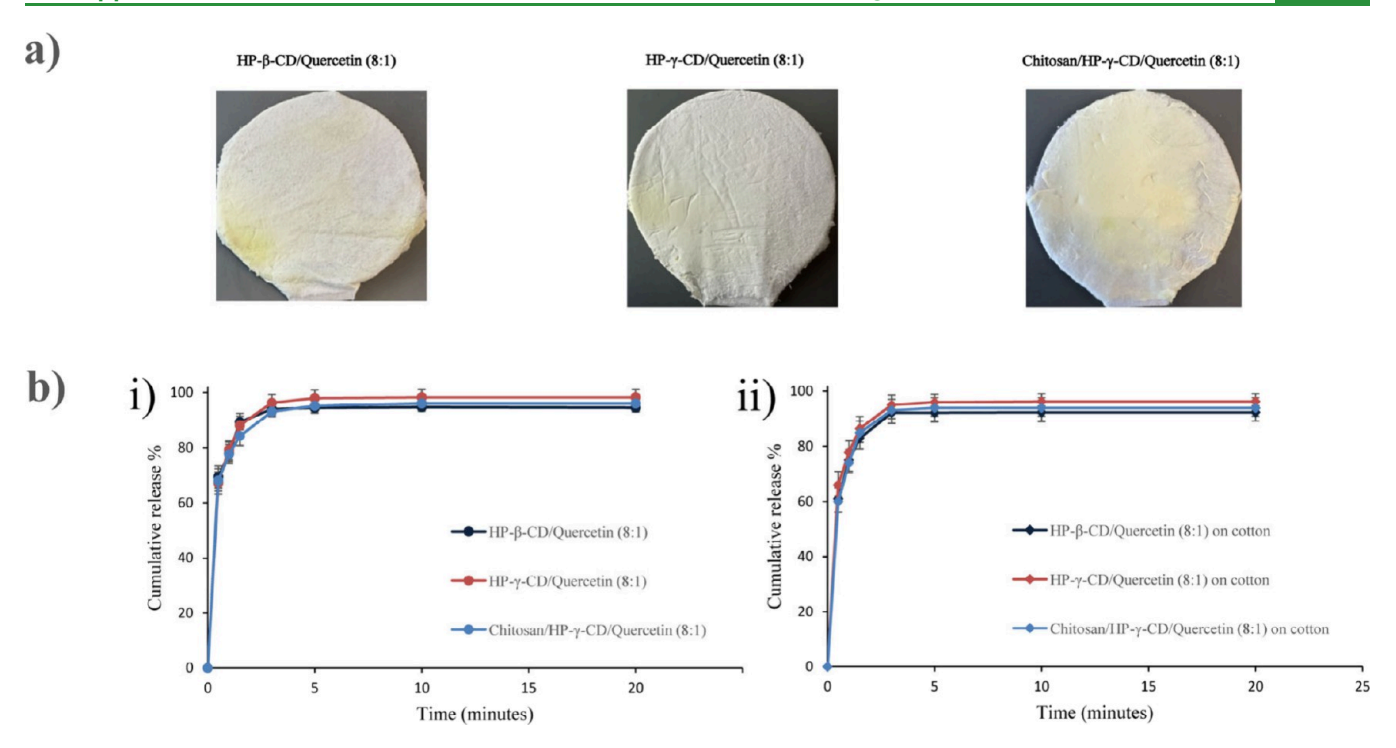


Figure 13. (a) Pictures of cotton nonwoven coated with HP- β -CD/Quercetin (8:1), HP- γ -CD/Quercetin (8:1), and Chitosan/HP- γ -CD/Quercetin (8:1). (b) Time-dependent release profiles of nanofibers (i) in free-standing form and (ii) coated on cotton nonwoven.

forming a more stable complex due to a better size match. The CD/Quercetin inclusion complexes were electrospun to develop smooth nanofibers. The DSC, TGA, and XRD characterizations further confirmed the formation of inclusion complexation and the suitability of HP-y-CD to form a more stable complex. The loading efficiency tests and ¹H NMR characterization demonstrated a near-complete loading efficiency, indicating minimal quercetin loss during the process. The release study also showed that the nanofibers both in freestanding form and coated on cotton followed a similar fastreleasing profile in the first 3 min due to their fast dissolution. These results demonstrate the ability of this coating to deliver a significant quercetin content. Moreover, to analyze the performance of wound dressing, the antibacterial and antioxidant properties were investigated. Quercetin is known for its excellent antioxidant properties, and the antioxidant investigation showed that the inclusion complexation resulted in a significantly higher antioxidant activity compared with that of quercetin powder. Due to employing all-natural materials, the nanofibers were well-tolerated by cells. The results showed improving quercetin solubility leads to comprehensive antiinflammatory properties against immune and regenerative cells, providing a suitable environment for wound healing, particularly for chronic wounds. This result suggests that upon coating onto cotton, the nanofibrous coating can provide excellent antioxidant and anti-inflammatory activities, providing swift and effective wound healing. Aiding from quercetin's biological properties, the nanofibers also showed suitable antibacterial activity against Escherichia coli and Staphylococcus aureus bacteria. This effect was further improved by the inclusion of chitosan, as it resulted in the complete removal of the bacterial colonies. Therefore, the prepared nanofibers with their excellent antibacterial activity can present themselves as a biofunctional coating to prevent wound infection.

AUTHOR INFORMATION

Corresponding Author

Tamer Uyar — Fiber Science Program, Department of Human Centered Design, College of Human Ecology, Cornell University, Ithaca, New York 14853, United States; orcid.org/0000-0002-3989-4481; Phone: +1 (607) 255-4658; Email: tu46@cornell.edu

Authors

Mohsen Alishahi – Fiber Science Program, Department of Human Centered Design, College of Human Ecology, Cornell University, Ithaca, New York 14853, United States

Ruobai Xiao – Fiber Science Program, Department of Human Centered Design, College of Human Ecology, Cornell University, Ithaca, New York 14853, United States

Melisa Kreismanis – Fiber Science Program, Department of Human Centered Design, College of Human Ecology, Cornell University, Ithaca, New York 14853, United States

Rimi Chowdhury — Department of Population Medicine and Diagnostic Sciences, College of Veterinary Medicine, Cornell University, Ithaca, New York 14853, United States;

orcid.org/0000-0002-4530-0029

Mahmoud Aboelkheir — Fiber Science Program, Department of Human Centered Design, College of Human Ecology, Cornell University, Ithaca, New York 14853, United States; orcid.org/0000-0002-4051-7253

Serafina Lopez – Nancy E. and Peter C. Meinig School of Biomedical Engineering, Cornell University, Ithaca, New York 14853, United States; orcid.org/0000-0001-7117-5156

Craig Altier – Department of Population Medicine and Diagnostic Sciences, College of Veterinary Medicine, Cornell University, Ithaca, New York 14853, United States

Lawrence J. Bonassar – Nancy E. and Peter C. Meinig School of Biomedical Engineering and Sibley School of Mechanical and Aerospace Engineering, Cornell University, Ithaca, New

York 14853, United States; oorcid.org/0000-0003-1094-6433

Hongqing Shen — Cotton Incorporated, Cary, North Carolina 27513, United States

Complete contact information is available at: https://pubs.acs.org/10.1021/acsabm.4c00751

Author Contributions

M.A. (Mohsen Alishahi): conceptualization, methodology, investigation, writing of the original draft, and review and editing. R.X. and M.K.: investigation. R.C.: investigation of the antibacterial and anti-inflammatory tests and editing. M.A. (Mahmoud Aboelkheir): investigation of the 2D-NMR part. S.G.L.: participated in the investigation for the MTT assay. C.A.: supervision and resources for antibacterial and anti-inflammatory tests. L.J.B.: supervision and resources for the MTT assay. H.S.: conceptualization and editing. T.U.: supervised the study and participated in funding acquisition, project administration, conceptualization, formal analysis, methodology, and review and editing.

Funding

This research was funded by Cotton Incorporated (Cary, NC, USA), Project No. 23-887.

Notes

The authors declare no competing financial interest.

ACKNOWLEDGMENTS

This work made use of the Cornell Center for Materials Research Shared Facilities, which are supported through the NSF MRSEC program (DMR-1719875), the Cornell Chemistry NMR Facility supported in part by the NSF MRI program (CHE-1531632), and the Department of Human Centered Design facilities. Freepik and Vecteezy.com figures were used as parts for the design of Figure ¹.

REFERENCES

- (1) Jin, Y.; Wang, C.; Xia, Z.; Niu, P.; Li, Y.; Miao, W. Photodynamic Chitosan Sponges with Dual Instant and Enduring Bactericidal Potency for Treating Skin Abscesses. *Carbohydr. Polym.* **2023**, *306*, No. 120589.
- (2) Liang, Y.; He, J.; Guo, B. Functional Hydrogels as Wound Dressing to Enhance Wound Healing. *ACS Nano* **2021**, *15* (8), 12687–12722.
- (3) Pinho, E.; Soares, G. Functionalization of Cotton Cellulose for Improved Wound Healing. *J. Mater. Chem. B* **2018**, *6* (13), 1887–1898.
- (4) Liu, C.; Ling, J.; Yang, L.-Y.; Ouyang, X.-k.; Wang, N. Chitosan-Based Carbon Nitride-Polydopamine-Silver Composite Dressing with Antibacterial Properties for Wound Healing. *Carbohydr. Polym.* **2023**, 303, No. 120436.
- (5) Davani, F.; Alishahi, M.; Sabzi, M.; Khorram, M.; Arastehfar, A.; Zomorodian, K. Dual Drug Delivery of Vancomycin and Imipenem/Cilastatin by Coaxial Nanofibers for Treatment of Diabetic Foot Ulcer Infections. *Materials Science and Engineering:* C 2021, 123, No. 111975.
- (6) Priya, S.; Choudhari, M.; Tomar, Y.; Desai, V. M.; Innani, S.; Dubey, S. K.; Singhvi, G. Exploring Polysaccharide-Based Bio-Adhesive Topical Film as a Potential Platform for Wound Dressing Application: A Review. *Carbohydr. Polym.* **2024**, 327, No. 121655.
- (7) Montaser, A. S.; Rehan, M.; El-Senousy, W. M.; Zaghloul, S. Designing Strategy for Coating Cotton Gauze Fabrics and Its Application in Wound Healing. *Carbohydr. Polym.* **2020**, 244, No. 116479.

- (8) Hebeish, A.; Sharaf, S. Novel Nanocomposite Hydrogel for Wound Dressing and Other Medical Applications. *RSC Adv.* **2015**, 5 (125), 103036–103046.
- (9) Li, Z.; Milionis, A.; Zheng, Y.; Yee, M.; Codispoti, L.; Tan, F.; Poulikakos, D.; Yap, C. H. Superhydrophobic Hemostatic Nanofiber Composites for Fast Clotting and Minimal Adhesion. *Nat. Commun.* **2019**, *10* (1), 5562.
- (10) Alishahi, M.; Aboelkheir, M.; Chowdhury, R.; Altier, C.; Shen, H.; Uyar, T. Functionalization of Cotton Nonwoven with Cyclodextrin/Lawsone Inclusion Complex Nanofibrous Coating for Antibacterial Wound Dressing. *Int. J. Pharm.* **2024**, *652*, No. 123815.
- (11) Rezaei, M.; Davani, F.; Alishahi, M.; Masjedi, F. Updates in Immunocompatibility of Biomaterials: Applications for Regenerative Medicine. *Expert Review of Medical Devices* **2022**, *19* (4), 353–367.
- (12) Yu, B.; He, C.; Wang, W.; Ren, Y.; Yang, J.; Guo, S.; Zheng, Y.; Shi, X. Asymmetric Wettable Composite Wound Dressing Prepared by Electrospinning with Bioinspired Micropatterning Enhances Diabetic Wound Healing. ACS Applied Bio Materials 2020, 3 (8), 5383–5394.
- (13) Singh, B.; Kim, J.; Shukla, N.; Lee, J.; Kim, K.; Park, M.-H. Smart Delivery Platform Using Core—Shell Nanofibers for Sequential Drug Release in Wound Healing. ACS Applied Bio Materials 2023, 6 (6), 2314–2324.
- (14) Teodoro, K. B. R.; Alvarenga, A. D.; Rocha Oliveira, L. F.; Marques Chagas, P. A.; Lopes, R. G.; Andre, R. d. S.; Mercante, L. A.; Alves, F.; Stringasci, M. D.; Buzza, H. H.; Inada, N. M.; Correa, D. S. Fast Fabrication of Multifunctional Pcl/Curcumin Nanofibrous Membranes for Wound Dressings. *ACS Applied Bio Materials* **2023**, 6 (6), 2325–2337.
- (15) Watson, A. L.; Eckhart, K. E.; Wolf, M. E.; Sydlik, S. A. Hyaluronic Acid-Based Antibacterial Hydrogels for Use as Wound Dressings. *ACS Applied Bio Materials* **2022**, *5* (12), 5608–5616.
- (16) Gaspar-Pintiliescu, A.; Stanciuc, A.-M.; Craciunescu, O. Natural Composite Dressings Based on Collagen, Gelatin and Plant Bioactive Compounds for Wound Healing: A Review. *Int. J. Biol. Macromol.* **2019**, *138*, 854–865.
- (17) Gorain, B.; Pandey, M.; Leng, N. H.; Yan, C. W.; Nie, K. W.; Kaur, S. J.; Marshall, V.; Sisinthy, S. P.; Panneerselvam, J.; Molugulu, N.; et al. Advanced Drug Delivery Systems Containing Herbal Components for Wound Healing. *Int. J. Pharm.* **2022**, *617*, No. 121617.
- (18) Ulusoy, H. G.; Sanlier, N. A Minireview of Quercetin: From Its Metabolism to Possible Mechanisms of Its Biological Activities. *Critical Reviews in Food Science and Nutrition* **2020**, *60* (19), 3290–3303.
- (19) Azzi, J.; Jraij, A.; Auezova, L.; Fourmentin, S.; Greige-Gerges, H. Novel Findings for Quercetin Encapsulation and Preservation with Cyclodextrins, Liposomes, and Drug-in-Cyclodextrin-in-Liposomes. *Food Hydrocolloids* **2018**, *81*, 328–340.
- (20) Mansi, K.; Kumar, R.; Narula, D.; Pandey, S. K.; Kumar, V.; Singh, K. Microwave-Induced Cuo Nanorods: A Comparative Approach between Curcumin, Quercetin, and Rutin to Study Their Antioxidant, Antimicrobial, and Anticancer Effects against Normal Skin Cells and Human Breast Cancer Cell Lines Mcf-7 and T-47d. ACS Applied Bio Materials 2022, 5 (12), 5762–5778.
- (21) Zhu, X.; Li, N.; Wang, Y.; Ding, L.; Chen, H.; Yu, Y.; Shi, X. Protective Effects of Quercetin on Uvb Irradiation-Induced Cytotoxicity through Ros Clearance in Keratinocyte Cells. *Oncol. Rep.* **2017**, *37* (1), 209–218.
- (22) Kinaci, M. K.; Erkasap, N.; Kucuk, A.; Koken, T.; Tosun, M. Effects of Quercetin on Apoptosis, Nf-Kb and Nos Gene Expression in Renal Ischemia/Reperfusion Injury. *Experimental and Therapeutic Medicine* **2012**, 3 (2), 249–254.
- (23) Hung, C. H.; Chan, S. H.; Chu, P. M.; Tsai, K. L. Quercetin Is a Potent Anti-Atherosclerotic Compound by Activation of Sirt1 Signaling under Oxldl Stimulation. *Molecular Nutrition and Food Research* **2015**, *59* (10), 1905–1917.
- (24) Yang, J.; Lin, J.; Zhang, J.; Chen, X.; Wang, Y.; Shen, M.; Xie, J. Fabrication of Zein/Mesona Chinensis Polysaccharide Nanoparticles:

- Physical Characteristics and Delivery of Quercetin. ACS Applied Bio Materials 2022, 5 (4), 1817–1828.
- (25) Yu, W.; Zhu, Y.; Li, H.; He, Y. Injectable Quercetin-Loaded Hydrogel with Cartilage-Protection and Immunomodulatory Properties for Articular Cartilage Repair. *ACS Applied Bio Materials* **2020**, 3 (2), 761–771.
- (26) Gong, W.; Yang, W.; Zhou, J.; Zhang, S.; Yu, D.-G.; Liu, P. Engineered Beads-on-a-String Nanocomposites for an Improved Drug Fast-Sustained Bi-Stage Release. *Nanocomposites* **2024**, *10* (1), 240–253.
- (27) Chen, S.; Zhou, J.; Fang, B.; Ying, Y.; Yu, D. G.; He, H. Three Ehda Processes from a Detachable Spinneret for Fabricating Drug Fast Dissolution Composites. *Macromol. Mater. Eng.* **2024**, 309 (4), No. 2300361.
- (28) Sun, Y.; Zhou, J.; Zhang, Z.; Yu, D.-G.; Bligh, S. W. A. Integrated Janus Nanofibers Enabled by a Co-Shell Solvent for Enhancing Icariin Delivery Efficiency. *Int. J. Pharm.* **2024**, 658, No. 124180.
- (29) Topuz, F.; Uyar, T. Advances in the Development of Cyclodextrin-Based Nanogels/Microgels for Biomedical Applications: Drug Delivery and Beyond. *Carbohydr. Polym.* **2022**, 297, No. 120033.
- (30) Aytac, Z.; Kusku, S. I.; Durgun, E.; Uyar, T. Quercetin/B-Cyclodextrin Inclusion Complex Embedded Nanofibres: Slow Release and High Solubility. *Food Chem.* **2016**, *197*, 864–871.
- (31) Čelebioglu, A.; Uyar, T. Green Synthesis of Polycyclodextrin/ Drug Inclusion Complex Nanofibrous Hydrogels: Ph-Dependent Release of Acyclovir. ACS Applied Bio Materials **2023**, 6 (9), 3798–3809
- (32) Güleç, K.; Demirel, M. Characterization and Antioxidant Activity of Quercetin/Methyl-B-Cyclodextrin Complexes. *Curr. Drug Delivery* **2016**, 13 (3), 444–451.
- (33) Zhao, L.-J.; Yang, S.-L.; Jin, W.; Yang, H.-W.; Li, F.-Y.; Chi, S.-M.; Zhu, H.-Y.; Lei, Z.; Zhao, Y. Host-Guest Inclusion Systems of Morin Hydrate and Quercetin with Two Bis (B-Cyclodextrin) S: Preparation, Characterization, and Antioxidant Activity. *Aust. J. Chem.* 2019, 72 (6), 440–449.
- (34) Aytac, Z.; Ipek, S.; Durgun, E.; Uyar, T. Antioxidant Electrospun Zein Nanofibrous Web Encapsulating Quercetin/Cyclodextrin Inclusion Complex. *J. Mater. Sci.* **2018**, *53*, 1527–1539.
- (35) ISO 10993-5: Biological Evaluation of Medical Devices Part 5: Tests for in vitro cytotoxicity; International Organization for Standardization, 1999.
- (36) Wallin, R. F. In A Practical Guide to Iso 10993-12: Sample Preparation and Reference Materials; MDDI, Los Angeles, CA, USA, 1998.
- (37) Celebioglu, A.; Uyar, T. Fast-Dissolving Antioxidant Curcumin/Cyclodextrin Inclusion Complex Electrospun Nanofibrous Webs. *Food Chem.* **2020**, *317*, No. 126397.
- (38) Pittol, V.; Veras, K. S.; Doneda, E.; Silva, A. D.; Delagustin, M. G.; Koester, L. S.; Bassani, V. L. The Challenge of Flavonoid/ Cyclodextrin Complexation in a Complex Matrix of the Quercetin, Luteolin, and 3-O-Methylquercetin. *Pharm. Dev. Technol.* **2022**, 27 (6), 625–634.
- (39) Haouas, M.; Falaise, C.; Leclerc, N.; Floquet, S.; Cadot, E. Nmr Spectroscopy to Study Cyclodextrin-Based Host-Guest Assemblies with Polynuclear Clusters. *Dalton Transactions* **2023**, *52*, 13467.
- (40) Eskitoros-Togay, Ş. M.; Bulbul, Y. E.; Dilsiz, N. Quercetin-Loaded and Unloaded Electrospun Membranes: Synthesis, Characterization and in Vitro Release Study. *Journal of Drug Delivery Science and Technology* **2018**, *47*, 22–30.
- (41) Ezati, P.; Rhim, J.-W. Fabrication of Quercetin-Loaded Biopolymer Films as Functional Packaging Materials. *ACS Applied Polymer Materials* **2021**, 3 (4), 2131–2137.
- (42) Xu, Y.; Xu, Y.; Sun, C.; Zou, L.; He, J. The Preparation and Characterization of Plasticized Pva Fibres by a Novel Glycerol/Pseudo Ionic Liquids System with Melt Spinning Method. *Eur. Polym. J.* **2020**, *133*, No. 109768.

- (43) Topuz, F.; Uyar, T. Influence of Hydrogen-Bonding Additives on Electrospinning of Cyclodextrin Nanofibers. *ACS Omega* **2018**, 3 (12), 18311–18322.
- (44) Saokham, P.; Loftsson, T. Γ-Cyclodextrin. Int. J. Pharm. 2017, 516 (1), 278–292.
- (45) Manna, S.; Seth, A.; Gupta, P.; Nandi, G.; Dutta, R.; Jana, S.; Jana, S. Chitosan Derivatives as Carriers for Drug Delivery and Biomedical Applications. ACS Biomaterials Science & Engineering 2023, 9 (5), 2181–2202.
- (46) Mukhopadhyay, P.; Maity, S.; Mandal, S.; Chakraborti, A. S.; Prajapati, A. K.; Kundu, P. P. Preparation, Characterization and in Vivo Evaluation of Ph Sensitive, Safe Quercetin-Succinylated Chitosan-Alginate Core-Shell-Corona Nanoparticle for Diabetes Treatment. *Carbohydr. Polym.* **2018**, *182*, 42–51.
- (47) da Costa, E. M.; Filho, J. M. B.; do Nascimento, T. G.; Macêdo, R. O. Thermal Characterization of the Quercetin and Rutin Flavonoids. *Thermochim. Acta* **2002**, 392–393, 79–84.
- (48) Long, J.; Etxeberria, A. E.; Kornelsen, C.; Nand, A. V.; Ray, S.; Bunt, C. R.; Seyfoddin, A. Development of a Long-Term Drug Delivery System with Levonorgestrel-Loaded Chitosan Microspheres Embedded in Poly(Vinyl Alcohol) Hydrogel. *ACS Applied Bio Materials* **2019**, 2 (7), 2766–2779.
- (49) Celebioglu, A.; Saporito, A. F.; Uyar, T. Green Electrospinning of Chitosan/Pectin Nanofibrous Films by the Incorporation of Cyclodextrin/Curcumin Inclusion Complexes: Ph-Responsive Release and Hydrogel Features. ACS Sustainable Chem. Eng. 2022, 10 (14), 4758–4769.
- (50) Asgari, Q.; Alishahi, M.; Davani, F.; Caravan, D.; Khorram, M.; Enjavi, Y.; Barzegar, S.; Esfandiari, F.; Zomorodian, K. Fabrication of Amphotericin B-Loaded Electrospun Core—Shell Nanofibers as a Novel Dressing for Superficial Mycoses and Cutaneous Leishmaniasis. *Int. J. Pharm.* **2021**, *606*, No. 120911.
- (51) Fitzmaurice, S.; Sivamani, R.; Isseroff, R. Antioxidant Therapies for Wound Healing: A Clinical Guide to Currently Commercially Available Products. *Skin Pharmacology and Physiology* **2011**, 24 (3), 113–126.
- (52) Jin, X.; Su, R.; Li, R.; Song, L.; Chen, M.; Cheng, L.; Li, Z. Amelioration of Particulate Matter-Induced Oxidative Damage by Vitamin C and Quercetin in Human Bronchial Epithelial Cells. *Chemosphere* **2016**, *144*, 459–466.
- (53) Chen, H.; Lu, C.; Liu, H.; Wang, M.; Zhao, H.; Yan, Y.; Han, L. Quercetin Ameliorates Imiquimod-Induced Psoriasis-Like Skin Inflammation in Mice Via the Nf-Kb Pathway. *International Immunopharmacology* **2017**, *48*, 110–117.
- (54) Karuppannan, S. K.; Dowlath, M. J. H.; Ramalingam, R.; Musthafa, S. A.; Ganesh, M. R.; Chithra, V.; Ravindran, B.; Arunachalam, K. D. Quercetin Functionalized Hybrid Electrospun Nanofibers for Wound Dressing Application. *Materials Science and Engineering: B* **2022**, 285, No. 115933.
- (55) Wang, Z.; Zhang, G.; Le, Y.; Ju, J.; Zhang, P.; Wan, D.; Zhao, Q.; Jin, G.; Su, H.; Liu, J.; Feng, J.; Fu, Y.; Hou, R. Quercetin Promotes Human Epidermal Stem Cell Proliferation through the Estrogen Receptor/B-Catenin/C-Myc/Cyclin A2 Signaling Pathway. *Acta Biochimica et Biophysica Sinica* **2020**, 52 (10), 1102–1110.
- (56) Adamczak, A.; Ożarowski, M.; Karpiński, T. M. Antibacterial Activity of Some Flavonoids and Organic Acids Widely Distributed in Plants. *Journal of Clinical Medicine* **2020**, 9 (1), 109.
- (57) Cushnie, T. T.; Lamb, A. J. Antimicrobial Activity of Flavonoids. *Int. J. Antimicrob. Agents* **2005**, *26* (5), 343–356.
- (58) Wang, S.; Yao, J.; Zhou, B.; Yang, J.; Chaudry, M. T.; Wang, M.; Xiao, F.; Li, Y.; Yin, W. Bacteriostatic Effect of Quercetin as an Antibiotic Alternative in Vivo and Its Antibacterial Mechanism in Vitro. *Journal of Food Protection* **2018**, *81* (1), 68–78.
- (59) Roy, S.; Rhim, J.-W. Fabrication of Chitosan-Based Functional Nanocomposite Films: Effect of Quercetin-Loaded Chitosan Nanoparticles. *Food Hydrocolloids* **2021**, *121*, No. 107065.
- (60) Simon, A. T.; Dutta, D.; Chattopadhyay, A.; Ghosh, S. S. Quercetin-Loaded Luminescent Hydroxyapatite Nanoparticles for Theranostic Application in Monolayer and Spheroid Cultures of

- Cervical Cancer Cell Line in Vitro. ACS Applied Bio Materials 2021, 4 (5), 4495–4506.
- (61) Xia, H.; Hu, Q.; Yang, Y.; Yuan, H.; Cai, Y.; Liu, Z.; Xu, Z.; Xiong, Y.; Zhou, J.; Ye, Q.; Zhong, Z. Effect of Matrix Metalloproteinase 23 Accelerating Wound Healing Induced by Hydroxybutyl Chitosan. ACS Applied Bio Materials 2023, 6 (4), 1460–1470.
- (62) Krzyszczyk, P.; Schloss, R.; Palmer, A.; Berthiaume, F. The Role of Macrophages in Acute and Chronic Wound Healing and Interventions to Promote Pro-Wound Healing Phenotypes. *Frontiers in Physiology* **2018**, *9*, 419.
- (63) Aliyu, M.; Zohora, F. T.; Anka, A. U.; Ali, K.; Maleknia, S.; Saffarioun, M.; Azizi, G. Interleukin-6 Cytokine: An Overview of the Immune Regulation, Immune Dysregulation, and Therapeutic Approach. *International Immunopharmacology* **2022**, *111*, No. 109130. (64) Moodley, Y. P.; Misso, N. L.; Scaffidi, A. K.; Fogel-Petrovic, M.; McAnulty, R. J.; Laurent, G. J.; Thompson, P. J.; Knight, D. A. Inverse Effects of Interleukin-6 on Apoptosis of Fibroblasts from Pulmonary Fibrosis and Normal Lungs. *Am. J. Respir. Cell Mol. Biol.* **2003**, 29 (4), 490–498.
- (65) Liu, J.; Li, X.; Yue, Y.; Li, J.; He, T.; He, Y. The Inhibitory Effect of Quercetin on Il-6 Production by Lps-Stimulated Neutrophils. *Cellular and Molecular Immunology* **2005**, 2 (6), 455–460.
- (66) Chang, S.-H.; Lin, Y.-Y.; Wu, G.-J.; Huang, C.-H.; Tsai, G. J. Effect of Chitosan Molecular Weight on Anti-Inflammatory Activity in the Raw 264.7 Macrophage Model. *Int. J. Biol. Macromol.* **2019**, *131*, 167–175.
- (67) Liu, K.; Veenendaal, T.; Wiendels, M.; Ruiz-Zapata, A. M.; van Laar, J.; Kyranas, R.; Enting, H.; van Cranenbroek, B.; Koenen, H. J. P. M.; Mihaila, S. M.; et al. Synthetic Extracellular Matrices as a Toolbox to Tune Stem Cell Secretome. *ACS Appl. Mater. Interfaces* **2020**, *12* (51), 56723–56730.
- (68) Cialdai, F.; Risaliti, C.; Monici, M. Role of Fibroblasts in Wound Healing and Tissue Remodeling on Earth and in Space. Frontiers in Bioengineering and Biotechnology 2022, 10, No. 958381.
- (69) Jiang, L.; Yao, H.; Luo, X.; Zou, D.; Dai, S.; Liu, L.; Yang, P.; Zhao, A.; Huang, N. Polydopamine-Modified Copper-Doped Titanium Dioxide Nanotube Arrays for Copper-Catalyzed Controlled Endogenous Nitric Oxide Release and Improved Re-Endothelialization. ACS Applied Bio Materials 2020, 3 (5), 3123–3136.
- (70) García-Mediavilla, V.; Crespo, I.; Collado, P. S.; Esteller, A.; Sánchez-Campos, S.; Tuñón, M. J.; González-Gallego, J. The Anti-Inflammatory Flavones Quercetin and Kaempferol Cause Inhibition of Inducible Nitric Oxide Synthase, Cyclooxygenase-2 and Reactive C-Protein, and Down-Regulation of the Nuclear Factor Kappab Pathway in Chang Liver Cells. *Eur. J. Pharmacol.* **2007**, *557* (2–3), 221–229.